Since January 2020 Elsevier has created a COVID-19 resource centre with free information in English and Mandarin on the novel coronavirus COVID-19. The COVID-19 resource centre is hosted on Elsevier Connect, the company's public news and information website.

ADVANCES IN VIRUS RESEARCH, VOL 64

MOLECULAR INTERACTIONS IN THE ASSEMBLY OF CORONAVIRUSES

Cornelis A. M. de Haan and Peter J. M. Rottier

Virology Division, Department of Infectious Diseases and Immunology
Faculty of Veterinary Medicine, Utrecht University
3584 CL Utrecht, The Netherlands

I. Introduction

Viruses are multimolecular assemblies that range from small, regular, and simple to large, pleiomorphic, and complex. They consist of virus-specified proteins and nucleic acids and, in the case of enveloped viruses, of host-derived lipids. In infected cells the assembly of these different components into virions occurs with high precision amidst a huge background of tens of thousands of host compounds. Two key factors determine the efficiency of the assembly process: intracellular transport and molecular interactions.

Directional transport ensures the swift and accurate delivery of the virion components to the cellular compartment(s) where they must meet and form (sub)structures. Some viruses achieve this goal relatively simply when genome production occurs in close proximity

0065-3527/05 $35.00
DOI: 10.1016/S0065-3527(05)64006-7

to the virion assembly site (e.g., picornaviruses). Many viruses, however, have evolved more elaborate strategies. This is illustrated, for instance, by the α-herpesviruses. Assembly of these viruses starts in the nucleus by the encapsidation of viral DNA, using cytoplasmically synthesized capsid proteins; nucleocapsids then migrate to the cytosol, by budding at the inner nuclear membrane followed by deenvelopment, to pick up the tegument proteins. Subsequently, the tegumented capsids obtain their final envelope by budding into vesicles of the *trans*-Golgi network (TGN), where the viral envelope proteins have congregated after their synthesis in the endoplasmic reticulum; the assembled viral particles are finally released by fusion of the virion-containing vesicles with the plasma membrane. To achieve their transport goals viruses provide their components with address labels that can be read by the transport machinery of the cell. Once brought together, formation of the viral (sub)structures is governed and driven by their interactions. Whereas the assembly of nonenveloped viruses is generally restricted to the cell cytoplasm, although often in association with membranes, that of enveloped viruses involves multiple cellular compartments, as exemplified already for herpesviruses.

This review deals with the assembly of coronaviruses. We first describe what is known about the structure of the coronavirion and about the relevant properties of the structural components. We summarize the limited ultrastructural information about coronavirus assembly and budding. The main body of the review describes the interactions between the different structural components of the viruses and discusses their relevance for the process of virion formation. This review has a limited scope; for further information about other aspects of coronavirus biology the reader is referred to other reviews (de Vries *et al.*, 1997; Enjuanes *et al.*, 2001; Gallagher and Buchmeier, 2001; Holmes, 2001; Holmes *et al.*, 2001; Lai, 1997; Lai and Cavanagh, 1997; Lai *et al.*, 1994; Masters, 1999; Perlman, 1998; Rossen *et al.*, 1995; Sawicki and Sawicki, 1998; Siddell, 1995; Ziebuhr *et al.*, 2000).

II. Structure of the Coronavirion and Its Components

Coronaviruses are a group of enveloped, plus-stranded RNA viruses presently classified as a genus, which, together with the genus *Torovirus*, constitutes the family *Coronaviridae*. These viruses are grouped with two other families, the *Arteriviridae* and the *Roniviridae*, into the order *Nidovirales*. This classification is not based on structural

similarities—in fact, structure and composition of the viruses from the different families differ significantly—but on common features of genome organization and gene expression (de Vries *et al.*, 1997; Lai and Cavanagh, 1997).

Coronaviruses infect a wide variety of mammals as well as avian species (Table I). In general they cause respiratory or intestinal infections, but some coronaviruses can also infect other organs (liver, kidney, and brain). Until recently, these viruses were mainly of veterinary importance. This situation has changed quite dramatically because of the emergence of severe acute respiratory syndrome-

TABLE I
CORONAVIRUS GROUPS, THEIR MAIN REPRESENTATIVES, HOSTS, AND PRINCIPAL ASSOCIATED DISEASES

Group	Virus	Host	Disease
1	Feline coronavirus (FCoV)	Cat	Respiratory infection/enteritis/ peritonitis/systemic enteritis
	Canine coronavirus (CCoV)	Dog	Enteritis
	Transmissible gastroenteritis virus (TGEV)	Pig	Enteritis
	Porcine epidemic diarrhea virus (PEDV)	Pig	Enteritis
	Porcine respiratory coronavirus (PRCoV)	Pig	Respiratory infection
	Human coronavirus (HCoV)-NL63	Human	Respiratory infection
	Human coronavirus (HCoV)-229E	Human	Respiratory infection
2	Murine hepatitis virus (MHV)	Mouse	Respiratory infection/enteritis/ hepatitis/encephalitis
	Rat coronavirus (RCoV)	Rat	Respiratory infection
	Bovine coronavirus (BCoV)	Cow	Respiratory infection/enteritis
	Hemagglutinating encephalomyelitis virus (HEV)	Pig	Enteritis
	Human coronavirus (HCoV)-OC43	Human	Respiratory infection
3	Infectious bronchitis virus (IBV)	Chicken	Respiratory infection/enteritis
	Turkey coronavirus (TCoV)	Turkey	Enteritis
?	Severe acute respiratory syndrome-associated coronavirus (SARS-CoV)	Human	Respiratory infection/enteritis

associated coronavirus (SARS-CoV) in late 2002, which emphasized the potential relevance of coronaviruses for humans. On the basis of antigenic and genetic relationships the coronaviruses have been subdivided into three groups (Table I); the taxonomic position of SARS-CoV has not been formally assigned.

A. Coronavirion

Coronavirus particles have a typical appearance under the electron microscope. By the characteristic, approximately 20-nm-long spikes that emanate from their envelope the viruses acquire the solar image to which they owe their name (Fig. 1). The 80- to 120-nm virions have a pleiomorphic appearance that, whether artifact or real, reflects a pliable constellation, a feature that has severely hampered the ultrastructural analysis of these viruses. Hence, our knowledge about the structure of coronaviruses is still rudimentary.

The schematic representation of the current model of the coronavirion drawn in Fig. 1 is based on morphological and biochemical

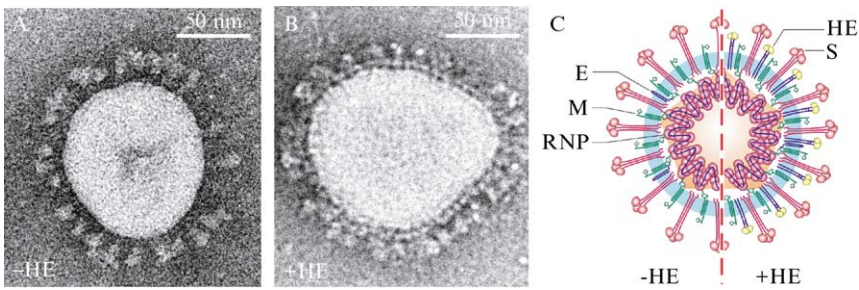

FIG 1. Electron micrographs of mouse hepatitis virus strain A59 (MHV-A59) virions without (A) and with (B) the hemagglutinin-esterase (HE) envelope protein (viruses kindly provided by R. de Groot, Virology Division, Utrecht University, The Netherlands; image courtesy of J. Lepault, VMS-CNRS, Gif-sur-Yvette, France). Large, club-shaped protrusions consisting of spike (S) protein trimers give the viruses their corona solis-like appearance. Viruses containing the HE protein display a second, shorter fringe of surface projections in addition to the spikes. (C) Schematic representation of the coronavirion. The viral RNA is encapsidated by the nucleocapsid (N) protein forming a helical ribonucleoprotein (RNP), which is in turn part of a structure with spherical, probably icosahedral, configuration. The nucleocapsid is surrounded by a lipid bilayer in which the S protein, the membrane glycoprotein (M), and the envelope protein (E) are anchored. In addition, some group 2 coronaviruses contain the HE protein in their lipid envelope as illustrated on the right side of the particle.

observations. As this picture illustrates, the particle consists of a nucleocapsid or core structure that is surrounded by a lipid envelope. Anchored in this envelope are the three canonical coronavirus membrane proteins: the membrane (M) protein, the envelope (E) protein, and the spike (S) protein. Viruses from group 2 have an additional, fourth membrane protein, the hemagglutinin-esterase (HE) protein. As a consequence these viruses display a second, shorter (5 nm) fringe of surface projections in addition to the spikes (Fig. 1B) (Bridger *et al.*, 1978; King *et al.*, 1985; Sugiyama and Amano, 1981).

The ribonucleoprotein (RNP) core contains one copy of the viral genomic RNA. This RNA is packaged into a helical structure by multiple copies of nucleocapsid protein (N). Size estimations of the flexible cylindrical structures varied quite considerably, ranging between 7 and 16 nm in diameter and up to 0.32 μm in length (see Laude and Masters, 1995). The ribonucleoprotein helix appears in turn to be contained within a spherical, probably icosahedral, configuration as indicated by various ultrastructural approaches using purified transmissible gastroenteritis virus (TGEV) and mouse hepatitis virus (MHV) (Risco *et al.*, 1996, 1998).

The molar ratio of the major structural proteins, S:N:M, has been variously estimated to be approximately 1:8:16 (Sturman *et al.*, 1980), 1:6:15 (Cavanagh, 1983a), 1:8:8 (Hogue and Brian, 1986), and 1:11:10 (Liu and Inglis, 1991), although an M:N molar ratio of 3 has also been reported (Escors *et al.*, 2001a). The S:HE molar ratio was estimated to be 4 (Hogue and Brian, 1986). The E protein is only a minor virion component and was calculated to occur in infectious bronchitis virus (IBV), TGEV, and MHV virions at a rate of approximately 100, 20, and 10 molecules per particle, respectively (Godet *et al.*, 1992; Liu and Inglis, 1991; Vennema *et al.*, 1996).

The lipid composition of coronaviral envelopes has been studied only to a limited extent. Comparison of the phospholipid composition of MHV with that of its host cell showed increased levels of sphingomyelin, phosphatidylserine, and phosphatidylinositol and a decrease in the level of phosphatidylethanolamine (van Genderen *et al.*, 1995). Whether the lipid composition of MHV is an accurate reflection of its budding compartment or whether certain lipids become enriched in the virus during budding is not known.

What follows is a general description of the individual virion components and their properties. This description is by no means complete as it is restricted to the information that is of relevance to the main topic of this review. For a schematic representation of the coronavirus life cycle see Fig. 2.

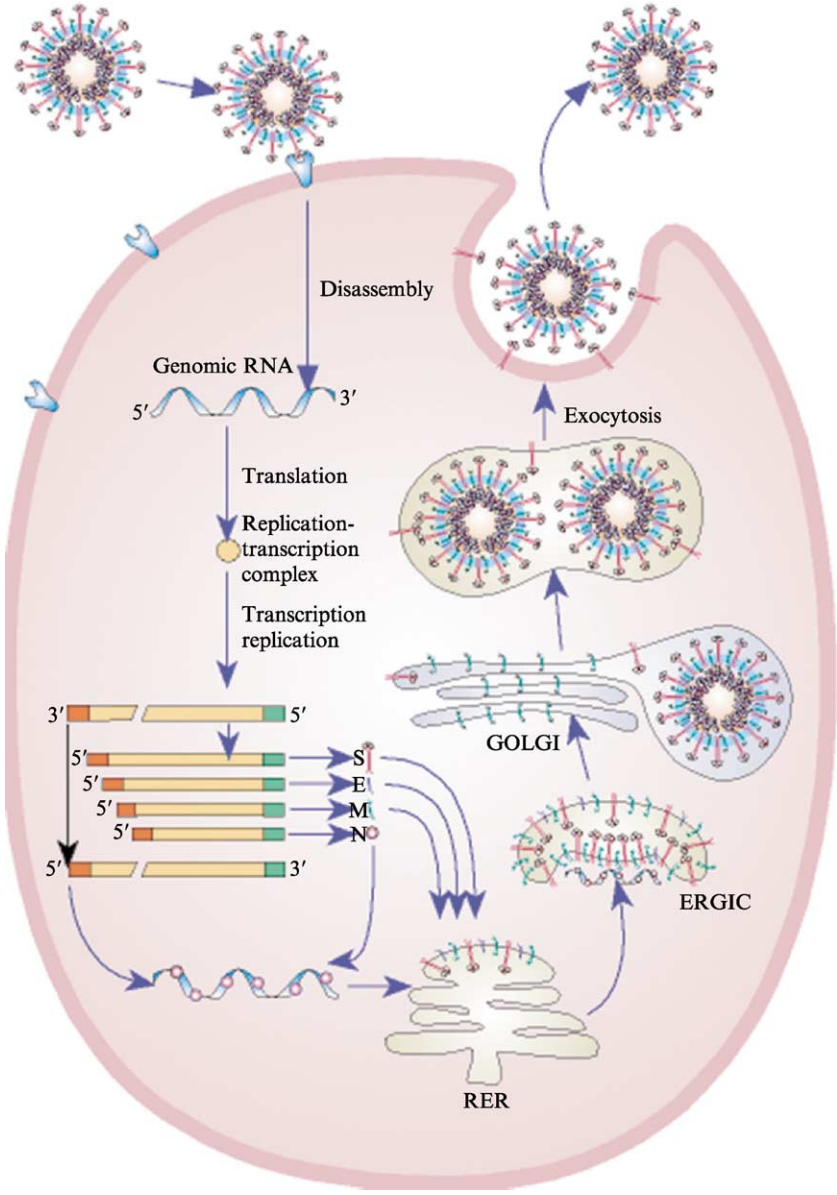

FIG 2. The coronavirus life cycle. The replication cycle starts with attachment of the virion by its S protein, that is, through the S1 subunit thereof, to the receptors on the host cell. This interaction leads to fusion of the virus envelope with a cellular membrane,

B. Viral Genome

Coronaviruses contain a single-stranded positive-sense RNA genome of some 27 to 31 kilobases, the largest nonsegmented viral RNA genomes known. The RNA has a 5′-terminal cap and a 3′-terminal poly(A) tract. Both genomic termini contain untranslated regions (UTRs) of some 200–500 nucleotides that harbor several *cis*-acting sequences and structural elements functioning in viral replication and transcription. Coronaviruses have a typical genome organization characterized by the occurrence of a distinctive set of genes that are essential for viability and occur in a fixed order: 5′-polymerase (*pol*)-S-E-M-N-3′ (Fig. 3). The *pol* gene comprises approximately two-thirds of the genome, from which it is translated directly. It encodes two large precursors (Pol1a and Pol1ab), the many functional cleavage products of which are collectively responsible for RNA replication and transcription (for reviews on coronavirus transcription and replication see de Vries *et al*., 1997; Lai, 1997; Lai and Cavanagh, 1997; Lai *et al*., 1994; Sawicki and Sawicki, 1998; Ziebuhr *et al*., 2000). The more downstream *pol1b* gene is translated by translational readthrough,

for which the S2 subunit is responsible. From the genomic RNA that is released by disassembly of the incoming particle the *pol1a* and *pol1b* genes are translated, resulting in the production of two large precursors (Pol1a and Pol1ab), the many cleavage products of which collectively constitute the functional replication–transcription complex. Genes located downstream of the *pol1b* gene are expressed from a 3′-coterminal nested set of subgenomic (sg) mRNAs, each of which additionally contains a short 5′ leader sequence derived from the 5′ end of the genome (shown in red). Transcription regulatory sequences (TRSs) located upstream of each gene serve as signals for the transcription of the sgRNAs. The leader sequence is joined at a TRS to all genomic sequence distal to that TRS by discontinuous transcription, most likely during the synthesis of negative-strand sgRNAs. In most cases, only the 5′-most gene of each sgRNA is translated. Multiple copies of the N protein package the genomic RNA into a helical structure in the cytoplasm. The structural proteins S, M, and E are inserted into the membrane of the rough endoplasmic reticulum (RER), from where they are transported to the ER-to-Golgi intermediate compartment (ERGIC) to meet the nucleocapsid and assemble into particles by budding. The M protein plays a central role in this process through interactions with all viral assembly partners. It gives rise to the formation of the basic matrix of the viral envelope generated by homotypic, lateral interactions between M molecules, and it interacts with the envelope proteins E, S, and HE (if present), as well as with the nucleocapsid, thereby directing the assembly of the virion. Virions are transported through the constitutive secretory pathway out of the cell—the glycoproteins on their way being modified in their sugar moieties, whereas the S proteins of some but not all coronaviruses are cleaved into two subunits by furin-like enzymes (see text for references).

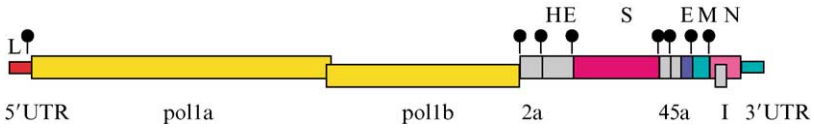

FIG 3. Coronavirus genome organization as illustrated for the group 2 virus MHV. The single-stranded, positive-sense RNA genome contains 5′- and 3′-terminal untranslated regions (UTRs) with a 5′-terminal cap and a 3′-terminal poly(A) tract. The leader sequence (L) in the 5′ UTR is indicated. All coronaviruses have their essential genes in the order 5′-*pol*-S-E-M-N-3′. The *pol1a* and *pol1b* genes comprise approximately two-thirds of the genome. The more downstream *pol1b* gene is translated by translational readthrough, using a ribosomal frameshift mechanism. Transcription regulatory sequences (TRSs) located upstream of each gene, which serve as signals for the transcription of the subgenomic (sg) RNAs, are indicated by circles. The genes encoding the structural proteins HE, S, E, M, and N are specified. Gray boxes indicate the accessory, group-specific genes, in the case of group 2 coronaviruses genes 2a, HE, 4, 5a, and I.

using a ribosomal frameshift mechanism for which a "slippery" sequence and a pseudoknot structure are required.

The genes located downstream of *pol1b* are expressed from a 3′-coterminal nested set of subgenomic (sg) RNAs, each of which additionally contains a short 5′ leader sequence derived from the 5′ end of the genome. Transcription regulatory sequences (TRSs) located upstream of each gene serve as signals for transcription of the sgRNAs. The leader sequence is joined at a TRS to all genomic sequence distal to that TRS by discontinuous transcription, most likely during the synthesis of negative-strand sgRNAs (Sawicki and Sawicki, 1998).

Besides the characteristic genes encoding the replicative and structural functions, coronaviruses have a more variable collection of additional genes that are located in two clusters in the 3′-terminal one-third of the genome. The genes differ distinctly in their nature and genomic position among the coronavirus groups, but they are specific for each group. These so-called group-specific genes appear not to be essential as shown by the occurrence of natural mutants defective in some of them (Brown and Brierley, 1995; Herrewegh *et al.*, 1995; Kennedy *et al.*, 2001; Luytjes, 1995; Shen *et al.*, 2003; Vennema, 1999; Vennema *et al.*, 1998; Woods, 2001) and by the observed viability of engineered deletion mutants lacking some or all of these genes (de Haan *et al.*, 2002b; Fischer *et al.*, 1997; Haijema *et al.*, 2004; Ortego *et al.*, 2003; Sola *et al.*, 2001). Except for the group 2-specific HE protein and, possibly, the poorly characterized I protein (Fischer *et al.*, 1997; Senanayake *et al.*, 1992), the latter encoded by an open reading frame completely contained within the N gene, the group-

specific proteins do not appear to occur in virions. Although their functions have not yet been resolved, mutant studies indicate that they play important roles in the interaction of coronaviruses with their host (de Haan *et al*., 2002b; Fischer *et al*., 1997; Haijema *et al*., 2004; Ortego *et al*., 2003).

C. N Protein

The N protein is the most abundantly expressed viral protein in infected cells (for a review, see Laude and Masters, 1995). Its size varies considerably between viruses from different groups (377–455 amino acids, i.e., molecular masses ranging between 45 and 60 kDa), N proteins from group 2 coronaviruses (Table I) being the largest. Whereas the amino acid sequences of N proteins are quite similar within the groups, the homology between proteins from different coronavirus groups is rather limited (30–35%). An exception is a region spanning about 50 residues within the amino-terminal one-third of the N molecule, where high sequence identity has been conserved across the different groups.

Despite the overall sequence variation the N proteins have a number of common characteristics. Consistent with their role as nucleic acid-binding proteins they are all highly basic because of the abundance of arginine and lysine residues. These are clustered mainly in two nearby regions in the middle of the molecules. The abundance of basic residues is reflected in the calculated overall isoelectric points of the N proteins, the values of which are in the range of 9.7–10.1. These numbers are the more significant in view of the acidic nature of the very carboxy-terminal domain; p*I* values ranging from 4.3 to 5.5 were calculated for the terminal 45 residues (Parker and Masters, 1990). Another general characteristic of the N proteins is their high content (7–11%) of serine residues, which are potential targets for phosphorylation. Although these residues occur all over the N molecule, their relative abundance within the first of the two basic regions is notable.

Little is known about the three-dimensional structure of the N protein. Of the SARS-CoV N protein the amino-terminal domain (residues 45–181) was analyzed by nuclear magnetic resonance spectroscopy. It appeared to consist of a five-stranded β sheet with a folding distinct from that of other RNA-binding proteins (Huang *et al*., 2004).

In coronavirus-infected cells the N protein can often be detected as one major and several minor forms, the latter polypeptides having a slightly lower molecular weight. The major species appeared to comigrate in gels with the N protein observed in virions, indicating that

only the full-length N species is incorporated into particles. How the minor N species arise and whether they are of particular significance for infection is unclear. They are most likely derived by proteolytic processing from the major N species. This is supported by studies from Eleouet *et al*. (2000), who showed the TGEV N protein to be cleaved by caspases. Caspase cleavage sites were also predicted in the carboxy terminus of several other coronavirus N proteins (Eleouet *et al*., 2000; Ying *et al*., 2004). These features are in agreement with observations showing that antibodies directed against the carboxy terminus of the MHV and TGEV N proteins were not reactive with the faster migrating electrophoretic forms. Furthermore, these smaller N protein forms appeared to be derived from the major species as judged from pulse–chase analyses (for a review see Laude and Masters, 1995).

The N protein is the only coronavirus structural protein known to become phosphorylated (for references see Laude and Masters, 1995). Both the major and minor N species appear to be phosphorylated as shown for MHV-A59 in Sac(−) cells (Rottier *et al*., 1981b) and for TGEV in LLC-PK1 cells (Garwes *et al*., 1984). Of the many potential target serines only a few are actually modified in the case of MHV (Stohlman and Lai, 1979; Wilbur *et al*., 1986). N protein phosphorylation does not seem to play a critical role in the regulation of virus assembly. In contrast, it has been hypothesized that dephosphorylation of the protein might facilitate disassembly during MHV cell entry (Kalicharran *et al*., 1996; Mohandas and Dales, 1991).

Immunofluorescence microscopy has shown the N protein to be localized in a particulate manner throughout the cytoplasm of coronavirus-infected cells. Although the protein lacks a membrane-spanning domain it was found in association with membranes (Anderson and Wong, 1993; Sims *et al*., 2000; Stohlman *et al*., 1983). For MHV, the N protein was found to colocalize partly with the membrane-associated viral replication complexes (Denison *et al*., 1999; van der Meer *et al*., 1999). In addition to its cytoplasmic localization, the N proteins of IBV, MHV, and TGEV have also been demonstrated to localize to the nucleolus both in coronavirus-infected cells and when expressed independently (Hiscox *et al*., 2001; Wurm *et al*., 2001). Putative nuclear localization signals were identified in these proteins. The IBV N protein was found to interact with nucleolar antigens, which appeared to occur more efficiently when the N protein was phosphorylated, and to affect the cell cycle (Chen *et al*., 2002). However, because MHV is able to replicate in enucleated cells (Brayton *et al*., 1981; Wilhelmsen *et al*., 1981) the nucleolar localization of the N protein does not appear an essential step during infection.

Although the primary function of the N protein is the formation of the viral ribonucleoprotein complex, several studies indicate the protein to be multifunctional. As indicated by its intracellular localization, the N protein is a likely component of the coronavirus replication and transcription complex. Its presence is not an absolute requirement for replication and transcription because a human coronavirus (HCoV) RNA vector containing the complete *pol1ab* gene appeared to be functional in the absence of the N protein (Thiel *et al.*, 2003). However, the efficiency of the system was much enhanced when the protein was present. Furthermore, using an *in vitro* system, it was demonstrated that antibodies to the N protein, but not those against the S and M proteins, inhibited viral RNA synthesis by 90% (Compton *et al.*, 1987). Interactions that have been observed between the N protein and leader/TRS sequences (Baric *et al.*, 1988; Nelson *et al.*, 2000; Stohlman *et al.*, 1988) and between N protein and the 3′ UTR (Zhou *et al.*, 1996) suggest a role for the N protein in the discontinuous transcription process. Furthermore, the N protein was also shown to interact with cellular proteins that play a role in coronavirus RNA replication and transcription (Choi *et al.*, 2002; Shi *et al.*, 2000). In addition, the N protein was reported to function as a translational enhancer of MHV sgRNAs (Tahara *et al.*, 1998).

D. M Protein

The M protein (previously known as E1 protein) is the most abundant envelope protein. It is the "building block" of the coronavirion and has been shown to interact with virtually every other virion component, as detailed in Section IV. The M protein is 221–230 residues in length, except for the group 1 M proteins, of which the amino terminus is about 30 residues longer. Despite large differences in primary sequences between M proteins from different antigenic groups, their hydropathicity profiles are remarkably similar. The M protein is highly hydrophobic. It has three hydrophobic domains alternating with short hydrophilic regions in the amino-terminal half of the protein, with the exception of the aforementioned group 1 M proteins, which have at their amino terminus a fourth hydrophobic domain that functions as a cleavable signal peptide. The carboxy-terminal half of the protein is amphipathic, with a short hydrophilic domain at the carboxy-terminal end (Fig. 4). In the center of the protein, directly adjacent to the third hydrophobic domain, is a stretch of eight amino acids that is well conserved (SWWSFNPE). The conservation of the overall chemical features suggests that there are rigid structural constraints on the

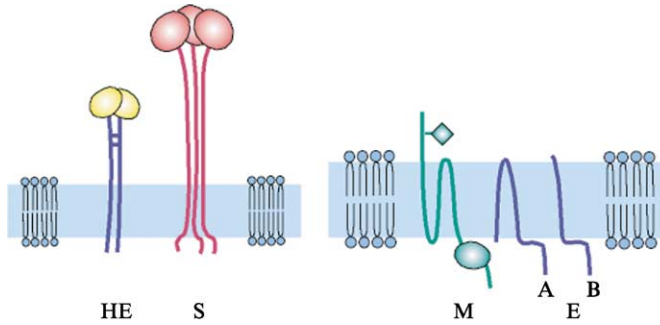

FIG 4. Membrane topology of the coronavirus envelope proteins. The HE and S proteins are both type I membrane proteins, with short carboxy-terminal cytoplasmic tails. The HE protein forms disulfide-linked homodimers, whereas the S protein forms noncovalently linked homotrimers. The S1 subunits presumably constitute the globular head, whereas the S2 subunits form the stalk-like region of the spike. The M protein spans the lipid bilayer three times, leaving a small amino-terminal domain in the lumen of intracellular organelles (or on the outside of the virion), whereas the carboxy-terminal half of the protein is located on the cytoplasmic side of the membrane (or inside the virion). In TGEV virions some of the M proteins have their cytoplasmic tail exposed on the outside (not shown). The M protein is glycosylated at its amino terminus (indicated by a diamond). The amphipathic domain of the M protein is represented by an oval. The hydrophilic carboxy terminus of the E protein is exposed on the cytoplasmic side of cellular membranes or on the inside of the virion. The E protein may span the bilayer once (b) or twice (a).

M protein as a result of functional requirements (for a review on the M protein, see Rottier, 1995).

Biochemical and theoretical studies led to a topological model for the MHV M protein (Armstrong *et al.*, 1984; Rottier *et al.*, 1984, 1986), in which the polypeptide spans the lipid bilayer three times, leaving a small amino-terminal domain (15–35 residues) in the lumen of intracellular organelles (or outside the virus), whereas the carboxy-terminal half of the protein is located on the cytoplasmic side of the membrane (or inside the virion). The lumenal domain and the hydrophilic carboxy terminus are susceptible to protease digestion and are thus exposed. The bulk of the carboxy-terminal half of the M protein is protease resistant, indicating that the amphipathic part of the protein is either folded tightly or embedded in the polar surface of the membrane. Indeed, a mutant lacking all three transmembrane domains was found to be associated with membranes (Mayer *et al.*, 1988). The model for the disposition of the M protein in the membrane was confirmed for IBV (Cavanagh *et al.*, 1986). Interestingly, the

M protein of TGEV was shown to adopt an additional conformation. In virions about one-third of the M molecules have their carboxy terminus exposed on the virus surface rather than buried inside the particle (Escors *et al*., 2001a; Risco *et al*., 1995). This appears to have immunological consequences (Risco *et al*., 1995) but the real significance of the dual topology is unclear. In MHV the M protein was found to assume only one defined membrane topology (Raamsman *et al*., 2000).

The coronavirus M protein is almost invariably glycosylated in its exposed amino-terminal domain. This provides the virion with a diffuse, hydrophilic cover on its outer surface. Whereas the group 1 and 3 coronaviruses and SARS-CoV all contain M proteins with only N-linked sugars, the M proteins of group 2 coronaviruses are O-glycosylated (for a review see Rottier, 1995). An exception is MHV-2, the M protein of which carries both O- and N-linked sugars (Yamada *et al*., 2000). N-Glycosylation is initiated in the endoplasmic reticulum by the cotranslational linkage of a large oligosaccharide structure to the polypeptide at asparagine residues within the consensus sequence NXS/T (where X is any amino acid). In contrast, mucin-type O-glycosylation starts posttranslationally with the addition of an *N*-acetylgalactosamine (GalNAc) monosaccharide to a hydroxylamino acid. O-Glycosylation is subsequently completed by stepwise addition of other monosaccharides such as galactose, *N*-acetylglucosamine, fucose, and sialic acid. MHV M proteins carry a well-conserved SS(X)TTXXP sequence at their extreme amino terminus. Despite the apparent presence of multiple hydroxylamino acids as potential oligosaccharide acceptor sites the M protein of MHV-A59 was found to be modified by the addition of only a single oligosaccharide side chain (de Haan *et al*., 1998b). This side chain, when studied in OST7-1 cells, appeared to be attached to the threonine at position 5. Mutation studies, however, revealed that alternative acceptor sites can also be used. No unique sequence motifs for O-glycosylation of MHV M could be identified, which is probably related to the occurrence in cells of multiple GalNAc transferases (de Haan *et al*., 1998b). As the expression of these enzymes varies in cells, conservation of the SS(X)TTXXP motif in MHV M protein may serve to increase opportunities for the protein to become glycosylated in different cell types.

The distinct conservation of N- and O-glycosylation among the M proteins of the different groups of coronaviruses suggests that the presence and the particular type of carbohydrates are somehow beneficial to the virus, most likely in its interaction with the host. Glycosylation of the M protein appeared not to be required for envelope assembly (de Haan *et al*., 1998a,) or for interaction with the S protein

(de Haan *et al.*, 1999), nor did it influence virus replication *in vitro* (de Haan *et al.*, 2002a, 2003; Laude *et al.*, 1992). Coronaviruses are able to induce interferon α (IFN-α) by their glycoproteins (Baudoux *et al.*, 1998a,b). For TGEV (Charley and Laude, 1988; Laude *et al.*, 1992) and MHV (de Haan *et al.*, 2003), the oligosaccharides linked to the M protein were demonstrated to be important for efficient IFN induction *in vitro*. The glycosylation status of the MHV M protein was found to influence the ability of the virus to replicate in the liver but not in the brain (de Haan *et al.*, 2003). Thus, viruses with N-glycosylated M proteins replicated to a significantly higher extent in liver than otherwise identical viruses carrying O-glycosylated M proteins. MHV with unglycosylated M proteins replicated to the lowest extent. The mechanism behind these observations remains to be elucidated.

When expressed in cells independently from the other viral proteins, the M proteins of MHV, IBV, TGEV, and feline coronavirus (FCoV) accumulate in the Golgi compartment, that is, beyond the site of virus budding (Klumperman *et al.*, 1994; Locker *et al.*, 1992; Machamer and Rose, 1987; Machamer *et al.*, 1990; Rottier and Rose, 1987), which is the intermediate compartment between the ER and the Golgi (ERGIC). The fine localization of the different proteins is, however, not the same. For instance, whereas the MHV M protein is concentrated in the *trans*-most Golgi compartments, the IBV M protein localizes to the *cis* side of the Golgi complex. Signals for localization appear to reside in the hydrophilic part of the cytoplasmic tail and in the transmembrane domains. The extreme carboxy-terminal tail of MHV M was shown to be necessary, although not sufficient, for Golgi localization (Armstrong and Patel, 1991; Locker *et al.*, 1994). Mutant proteins lacking this domain were transported to the plasma membrane. Also, mutation of a single tyrosine in this domain, which occurs in the context of a potential internalization signal, resulted in plasma membrane localization (C. A. M. de Haan and P. J. M. Rottier, unpublished results). The first transmembrane domain of the IBV M protein was shown to be required and sufficient for localization to the *cis*-Golgi region (Machamer and Rose, 1987; Machamer *et al.*, 1990, 1993; Swift and Machamer, 1991). This is not the case for the MHV M protein of which mutants with only the first transmembrane domain did not leave the ER (Armstrong *et al.*, 1990; Locker *et al.*, 1994; Rottier *et al.*, 1990). Moreover, insertion of the first transmembrane domain of MHV M into a reporter protein resulted in a chimeric protein that was transported to the cell surface (Armstrong and Patel, 1991; Machamer *et al.*, 1993), unlike a similar chimeric protein containing the first transmembrane domain of IBV that was retained in the Golgi

compartment (Machamer *et al*., 1993). Other MHV M mutant proteins lacking the first and second transmembrane domains were also not efficiently retained in the Golgi compartment and were diverted to endosomal structures (Armstrong *et al*., 1990; Locker *et al*., 1994). The mechanism by which Golgi retention of M proteins is regulated has not yet been resolved. However, oligomerization of the proteins, mediated by the transmembrane domains, seems to play an important role, perhaps in combination with retrieval mechanisms (de Haan *et al*., 2000; Maceyka and Machamer, 1997). Formation of oligomeric complexes has been demonstrated to correlate with Golgi retention of a reporter protein containing the first transmembrane domain of IBV M (Weisz *et al*., 1993) while also the Golgi-resident MHV M protein was found to occur in large, homomeric complexes (Locker *et al*., 1995). The lumenal domain of the M protein does not appear to contribute to localization; its deletion from MHV M did not affect the intracellular destination of the protein (Mayer *et al*., 1988; Rottier *et al*., 1990).

In infected cells the M proteins of IBV and MHV were observed to occur in the membranes of the budding compartment as well as in the Golgi compartment. Under these conditions their *cis–trans* distribution in the Golgi compartment was the same as when these proteins were expressed independently (Klumperman *et al*., 1994; Machamer *et al*., 1990).

E. E Protein

The E protein (previously known as sM protein) is a small protein (76–109 residues) and a minor component of the coronaviral envelope. Although the primary structures of E proteins are quite conserved within the different coronavirus groups, they share little homology between the groups. However, the proteins have several structural features in common. The E protein contains a relatively large hydrophobic region in its amino-terminal half, followed by a cysteine-rich region, an absolutely conserved proline residue, and a hydrophilic tail. E is an integral membrane protein, which is assembled in membranes without the involvement of a cleaved signal peptide (Raamsman *et al*., 2000). Its membrane topology has not been firmly established. Although the opposite was proposed initially for the TGEV E protein (Godet *et al*., 1992), there seems to be consensus about the hydrophilic carboxy terminus being exposed on the cytoplasmic side in cells or on the inside of the virion (Corse and Machamer, 2000; Raamsman *et al*., 2000). The amino terminus of the MHV E protein was not detectably present on the virion outside (Raamsman *et al*., 2000) but

appeared to be exposed cytoplasmically when it was extended with an amino-terminal epitope tag (Maeda *et al*., 2001), consistent with a topological model in which the hydrophobic domain spans the bilayer twice. For the IBV E protein evidence was provided indicating that the amino terminus is exposed lumenally in cells, consistent with a single spanning topology (Corse and Machamer, 2000) (Fig. 4).

The E protein is not glycosylated but appears to become palmitoylated. This was shown most convincingly for the IBV E protein by labeling with [^{3}H]palmitate (Corse and Machamer, 2002), both in IBV-infected cells and when the protein was expressed. Mutagenesis revealed that one or both of the two conserved cysteines became modified. The result is consistent with the observed increase in electrophoretic mobility of the MHV E protein after treatment with hydroxylamine, an agent that cleaves thioester-linked acyl chains (Yu *et al*., 1994). Others, however, were not able to confirm this post-translational modification (Godet *et al*., 1992; Raamsman *et al*., 2000).

In coronavirus-infected cells the E protein has been observed by immunofluorescence studies to occur at intracellular membranes as well as at the cell surface (Godet *et al*., 1992; Smith *et al*., 1990; Tung *et al*., 1992; Yu *et al*., 1994). When expressed exogenously from cDNA, the E protein was detected only in intracellular organelles, although at different locations. The MHV E protein localized to pre-Golgi membrane compartments, as was demonstrated by its colocalization with rab-1, a marker for the endoplasmic reticulum and the ERGIC, by electron microscopy (Raamsman *et al*., 2000). The IBV E protein, tagged at its amino terminus with an epitope, was also localized to pre-Golgi compartments (Lim and Liu, 2001). In another study, however, the IBV E protein was shown to accumulate in the Golgi apparatus, being distributed throughout the complex (Corse and Machamer, 2000, 2002). While the former study identified an ER-targeting signal in the extreme carboxy terminus of the E protein (Lim and Liu, 2001), the latter studies, using carboxy-terminal truncations, mapped the Golgi-targeting information to a region between tail residues 13 and 63 (Corse and Machamer, 2002). In addition, these authors showed the IBV E cytoplasmic tail to be necessary and sufficient for Golgi targeting.

The E protein was identified as a virion component relatively late, due to its low abundance and its small size (Godet *et al*., 1992; Liu and Inglis, 1991; Yu *et al*., 1994). It was estimated to occur in IBV, TGEV, and MHV virions at a rate of about 100, 20, and 10 molecules per particle, respectively (Godet *et al*., 1992; Liu and Inglis, 1991; Vennema *et al*., 1996). Because of its low abundance the E protein

may not have a genuine structural function in the virion envelope. Rather, it may have a morphogenetic function by taking strategic positions within the M protein lattice to generate the required membrane curvature. Alternatively, it may serve to close the neck of the budding particle as it pinches off the membrane (Vennema *et al.*, 1996). Expression of the E protein alone induced the formation of characteristic membrane structures also observed in infected cells, which apparently consist of masses of tubular, smooth convoluted membranes (David-Ferreira and Manaker, 1965; Raamsman *et al.*, 2000). In addition, it resulted in the formation of vesicles containing the E protein, shown to be released from the cells (Corse and Machamer, 2000; Maeda *et al.*, 1999).

MHV infection induces caspase-dependent apoptosis in some, but not all, cells. By expressing the viral structural proteins separately in cells, the activity could be attributed to the E protein (An *et al.*, 1999). Apoptosis induction has not been reported for E proteins from other coronaviruses.

Coronavirus E proteins share structural similarities with small hydrophobic membrane proteins found in other enveloped viruses. Examples are the Vpu protein of HIV-1, the 6K protein of alphaviruses, and the M2 protein of influenza virus. These proteins, also known as viroporins (Gonzalez and Carrasco, 2003), were demonstrated to modify membrane permeability and to help the efficient release of progeny virus.

F. S Protein

The S protein (previously known as E2) constitutes the spikes, the hallmark of coronaviruses under the electron microscope. It is the major determinant of host range, tissue tropism, pathogenesis, and virulence. It is a relatively large, 1160- to 1452-amino acid-long type I glycoprotein with a cleavable N-terminal signal sequence and a membrane-anchoring sequence followed by a short hydrophilic carboxy-terminal tail of about 30 residues (Fig. 4). When comparing primary sequences, the S protein shows two faces: an amino-terminal half with hardly any sequence similarities and a carboxy-terminal half in which regions with significant conservation can be observed (de Groot *et al.*, 1987a,b; for a review see Cavanagh, 1995), consistent with the distinctive functions of these domains (see later).

The S protein is synthesized as a heavily glycosylated polypeptide as demonstrated by the susceptibility of the glycans to endoglycosidases and by the dramatic effect of the N-glycosylation inhibitor tunicamycin.

The number of potential N-glycosylation sites ranges from 21 (MHV) to 35 [feline infectious peritonitis virus (FIPV)]. The S protein has not been reported to contain O-linked sugars. Cotranslational N-glycosylation is an essential requirement for proper folding, oligomerization, and transport of the S protein, as has also been shown for other (viral) glycoproteins (Doms *et al.*, 1993). Growth of coronaviruses in the presence of tunicamycin resulted in the production of spikeless, noninfectious particles (Holmes *et al.*, 1981; Mounir and Talbot, 1992; Rottier *et al.*, 1981a; Stern and Sefton, 1982). These particles were devoid of S protein, which was found to aggregate in the endoplasmic reticulum when glycosylation was inhibited (Delmas and Laude, 1990).

Folding of the S protein is a relatively slow process. Besides the addition of oligosaccharides it involves the formation and rearrangement of many intramolecular disulfide bonds. For the S protein of MHV-A59, the lumenal domain of which contains 42 cysteine residues, the major conformational events appear to take about 20 min during which the protein passes through a continuous spectrum of folding intermediates (Opstelten *et al.*, 1993a). Folding of S is probably the rate-limiting step in the process of oligomerization. Sufficiently folded S protein monomers associate in the endoplasmic reticulum to form trimers (Delmas and Laude, 1990; Lin *et al.*, 2004), with a half-time of approximately 1 h (Delmas and Laude, 1990; Vennema *et al.*, 1990a,b). Trimerization is likely to be required for export out of the endoplasmic reticulum. In infected cells S protein trimers interact with M protein (Opstelten *et al.*, 1995) and perhaps also with E protein, and migrate to the virus assembly site. A fraction of the S protein is transported to the plasma membrane where it can cause cell–cell fusion, a feature formally attributed to the S protein by its individual expression in cells (de Groot *et al.*, 1989; Pfleiderer *et al.*, 1990). Under such expression conditions the bulk of the S protein remains intracellularly (Vennema *et al.*, 1990a) in the endoplasmic reticulum (Opstelten *et al.*, 1995). Retrieval signals have been identified in the cytoplasmic tail of the S proteins from coronavirus groups 1 and 3 as well as in the tail of the SARS-CoV S protein, but not in the group 1 MHV S protein (Lontok *et al.*, 2004).

During its transport to the cell surface, either alone or as part of virions, the S protein undergoes further modifications. The N-linked sugars are modified and become mature during passage through the Golgi complex. The MHV S protein was shown to become palmitoylated, a modification that may already take place in the endoplasmic reticulum (van Berlo *et al.*, 1987). As a late step the S protein can be

cleaved. A basic amino acid sequence resembling the furin consensus sequence motif (RXR/KR) occurs approximately in the middle of the protein and was shown to be the target of a furin-like enzyme in the case of MHV-A59 (de Haan *et al.*, 2004). Cleavage has been demonstrated for S proteins from coronavirus groups 2 and 3, but not for S proteins from group 1 viruses (Cavanagh, 1995) or from SARS-CoV (Bisht *et al.*, 2004). The resulting amino-terminal S1 subunit and the membrane-anchored S2 subunit remain noncovalently linked. It has been suggested that the S1 subunit constitutes the globular head, whereas the S2 subunit forms the stalk-like region of the spike (Cavanagh, 1983b; de Groot *et al.*, 1987a,b).

The coronavirus S protein has two functions, which appear to be spatially separated. The S1 subunit (or the equivalent part in viruses with uncleaved S protein) is responsible for receptor binding, and the S2 subunit is responsible for membrane fusion. For several coronaviruses the receptor-binding site in S1 has been mapped. For MHV strain JHM (MHV-JHM), for instance, it was located in the domain composed of the amino-terminal 330 residues of the S molecule (Kubo *et al.*, 1994), residues 62–65 and 214–216 being particularly important (Saeki *et al.*, 1997; Suzuki and Taguchi, 1996). This amino-terminal domain also determined CEACAM1 receptor specificity of various MHV strains (Tsai *et al.*, 2003). For TGEV (Godet *et al.*, 1994), HCoV-229E (Bonavia *et al.*, 2003; Breslin *et al.*, 2003), and SARS-CoV (Babcock *et al.*, 2004; Wong *et al.*, 2004) the receptor-binding domains have also been mapped to the S1 subunit, although in different regions. In several cases neutralizing antibodies were demonstrated to bind the receptor-binding domains and to prevent the interaction with the receptor (Godet *et al.*, 1994; Kubo *et al.*, 1994; Sui *et al.*, 2004).

The interaction between the S protein and its receptor is the major determinant for virus entry and host range restriction. Nonpermissive cell lines can be rendered susceptible by making them express the receptor (see later references). Coronaviruses can also be retargeted to specific cells by exchanging the ectodomain of the S protein for that of an appropriate other coronavirus, as was demonstrated for MHV (Kuo *et al.*, 2000) and FIPV (Haijema *et al.*, 2003). Receptors have so far been identified for the group 2 coronavirus MHV (CEACAM; Dveksler *et al.*, 1991, 1993; Williams *et al.*, 1991); the group 1 coronaviruses TGEV and porcine respiratory coronavirus (PRCoV) (pAPN; Delmas *et al.*, 1992, 1993), FIPV (fAPN; Tresnan *et al.*, 1996), and HCoV-229E (hAPN; Yeager *et al.*, 1992); and for SARS-CoV (ACE2; Li *et al.*, 2003). The S proteins of the group 2 coronaviruses have been

observed to exhibit hemagglutinating activities. Although for bovine coronavirus (BCoV), HCoV-OC43, and hemagglutinating encephalomyelitis virus (HEV) 9-O-acetylated sialic acids were identified as a receptor determinant (Krempl *et al*., 1995; Kunkel and Herrler, 1993; Schultze and Herrler, 1992; Schultze *et al*., 1991a; Vlasak *et al*., 1988b), specific receptors for these viruses have not been identified. Also, the MHV S protein appears to bind sialic acid derivatives in addition to its specific receptor CEACAM, which may suggest that sialic acids function as an additional receptor determinant for MHV-like coronaviruses (Wurzer *et al*., 2002).

The ectodomain of the S2 subunit, which is involved in the fusion process, contains two heptad repeat (HR) regions (de Groot *et al*., 1987a,b), a sequence motif characteristic of coiled coils. Mutations in the first (i.e., membrane-distal) HR region of the MHV S protein resulted in fusion-negative phenotypes (Luo and Weiss, 1998) or in a low-pH dependence for fusion (Gallagher *et al*., 1991), whereas mutations in the second HR region caused defects in S protein oligomerization and fusion ability (Luo *et al*., 1999). A fusion peptide has not yet been identified in any of the coronavirus spike proteins, but is predicted to be located at (Bosch *et al*., 2004b; Chambers *et al*., 1990) or within (Luo and Weiss, 1998) the amino terminus of the first HR region. Binding of the S1 subunit to the (soluble) receptor, or exposure to 37 °C and an elevated pH, has been shown to trigger conformational changes that are supposed to facilitate virus entry by activation of the fusion function of the S2 subunit (Breslin *et al*., 2003; Gallagher, 1997; Lewicki and Gallagher, 2002; Matsuyama and Taguchi, 2002; Miura *et al*., 2004; Sturman *et al*., 1990; Taguchi and Matsuyama, 2002; Zelus *et al*., 2003). This conformational change is thought to lead to exposure of the fusion peptide and its interaction with the target membrane, further changes resulting in the formation of a heterotrimeric six-helix bundle, characteristic of class I viral fusion proteins, during the membrane fusion process. Indeed, peptides corresponding to the HR regions of MHV (Bosch *et al*., 2003; Xu *et al*., 2004) and SARS-CoV (Bosch *et al*., 2004b; Ingallinella *et al*., 2004; Liu *et al*., 2004; Tripet *et al*., 2004; Zhu *et al*., 2004) were found to assemble into stable oligomeric complexes in an antiparallel manner, which in the natural situation would result in the close colocation of the fusion peptide and the transmembrane domain. These peptides were further shown to be inhibitors for viral entry (Bosch *et al*., 2003, 2004b; Liu *et al*., 2004; Yuan *et al*., 2004; Zhu *et al*., 2004).

Besides the HR regions, other parts of the S protein are also likely to be important for the fusion process. All coronavirus S proteins contain

a highly conserved region (de Groot *et al*., 1987a), rich in aromatic residues, downstream of the second HR region, part of which may form the start of the transmembrane domain. The function of this domain is unknown, but a similar region in the HIV-1 Env protein was demonstrated to be important for viral fusion and Env incorporation into virions (Salzwedel *et al*., 1999). Immediately downstream of the transmembrane domain all S proteins contain a cysteine-rich region (de Groot *et al*., 1987a). Using a mutational approach including deletions, insertions, and substitutions, both the transmembrane domain and the cysteine-rich region immediately downstream thereof, but not the carboxy-terminal part of the cytoplasmic tail, were shown to be important for MHV S protein-induced cell–cell fusion (Bos *et al*., 1995; Chang and Gombold, 2001; Chang *et al*., 2000) (B. J. Bosch, C. A. M. de Haan, and P. J. M. Rottier, unpublished results).

The cleavage requirements of the S proteins for the biological activities of the coronavirus spike remain enigmatic. Whereas the S proteins of group 1 coronaviruses, such as FIPV (Vennema *et al*., 1990a), are not cleaved, those of other coronaviruses, particularly of groups 2 and 3, are cleaved to variable extents, depending on the viral strain and the cell type in which the viruses are grown (Frana *et al*., 1985; reviewed by Cavanagh, 1995). Cleavage of the S proteins is not required to expose the internal fusion peptide. Whereas cleavage of the MHV S protein generally correlates strongly with cell–cell fusion (Cavanagh, 1995), virus–cell fusion appeared not to be affected by preventing S protein cleavage, indicating that these fusion events have different requirements (de Haan *et al*., 2004). Similarly, whereas trypsin activation of SARS-CoV S protein was required for cell–cell fusion, it did not enhance the infectivity of cell-free pseudovirions (Simmons *et al*., 2004). For MHV-4, the spikes of which are able to initiate fusion without prior interaction with the primary MHV receptor (Gallagher *et al*., 1992), the stability of the S1–S2 heterodimers after S protein cleavage is low, allowing receptor-independent fusion. During cell culture adaptation, however, selected mutant viruses carried deletions in the S1 subunit, downstream of the receptor-binding domain, which resulted in stabilized S1–S2 heterodimers and receptor-dependent fusion activity (Krueger *et al*., 2001).

G. HE Protein

Virions of group 2 coronaviruses generally contain a fringe of shorter surface projections in addition to the characteristic spikes (Bridger *et al*., 1978; King *et al*., 1985; Sugiyama and Amano, 1981). These

viruses express and incorporate into their particles an additional membrane protein, HE (for a review see Brian *et al.*, 1995). Although all group 2 viruses contain an HE gene, the protein is not expressed by all MHV strains (Luytjes *et al.*, 1988; Yokomori *et al.*, 1991), indicating that HE is a nonessential protein also in these viruses.

The HE gene encodes a type I membrane protein of 424–439 residues that contains a cleavable signal peptide at its amino terminus (Hogue *et al.*, 1989; Kienzle *et al.*, 1990) and a transmembrane domain close to its carboxy terminus, leaving a short cytoplasmic tail of about 10 residues (Fig. 4). The ectodomain contains 8–10 putative N-linked glycosylation sites. The putative esterase active site (FGDS) is located near the (signal-cleaved) HE amino terminus. The coronavirus HE protein has 30% amino acid identity with the HE-1 subunit of the HE fusion protein of influenza C virus and the HE protein of torovirus (Cornelissen *et al.*, 1997). It has been suggested that coronaviruses have captured their HE module from influenza C virus or a related virus (Luytjes *et al.*, 1988). However, influenza C virus, toroviruses, and coronaviruses may well have acquired their HE sequences independently, not from each other but from yet another source (Cornelissen *et al.*, 1997). The HE protein becomes cotranslationally N-glycosylated when expressed in cells, giving rise to a polypeptide of approximately 60–65 kDa that rapidly forms disulfide-linked dimers (Hogue *et al.*, 1989; Kienzle *et al.*, 1990; King *et al.*, 1985; Parker *et al.*, 1989; Yokomori *et al.*, 1989; Yoo *et al.*, 1992). The HE dimers (or a higher order structure thereof) become incorporated into virions, while a proportion is transported to the cell surface (Kienzle *et al.*, 1990; Pfleiderer *et al.*, 1991).

Little is still known about the function(s) of the coronavirus HE protein. The protein contains hemagglutinin and acetyl esterase activities (Brian *et al.*, 1995). While the HE proteins of BCoV, HEV, and HCoV-OC43 hydrolyze the 9-*O*-acetyl group of sialic acid and therefore appear to function as receptor-destroying enzymes (Schultze *et al.*, 1991b; Vlasak *et al.*, 1988a), the HE proteins of MHV-like coronaviruses function as sialate-4-*O*-acetylesterases (Klausegger *et al.*, 1999; Regl *et al.*, 1999; Wurzer *et al.*, 2002). Although inhibition of the esterase activity of BCoV resulted in a 100- to 400-fold reduction in viral infectivity (Vlasak *et al.*, 1988a), it was shown both for BCoV and for an MHV strain expressing an HE gene that the S protein is required and sufficient for infection (Gagneten *et al.*, 1995; Popova and Zhang, 2002). In view of these results it has been proposed that the HE protein might play a role at an even earlier step and may mediate viral adherence to the intestinal wall through the specific yet reversible

binding to mucopolysaccharides. The process of binding to sialic acid receptors followed by cleavage and rebinding to intact receptors could theoretically result in virus motility and even allow migration through the mucus layer covering the epithelial target cells in the respiratory and enteric tracts (Cornelissen *et al*., 1997).

Several studies have indicated the HE protein to play a role in pathogenicity. The HE protein of BCoV (Deregt and Babiuk, 1987), but not that of MHV, was able to induce neutralizing antibodies. However, passive immunization of mice with nonneutralizing, MHV HE-specific antibodies protected the animals against a lethal MHV infection (Yokomori *et al*., 1992). Furthermore, intracerebral expression of the HE protein in mice was found to affect the neuropathogenicity of MHV (Yokomori *et al*., 1995; Zhang *et al*., 1998). Strikingly, HE protein-defective MHV mutants were rapidly selected during viral infection in the mouse brain (Yokomori *et al*., 1993), which may suggest that the HE protein plays a more critical role during the infection of other tissues.

III. Ultrastructural Observations of Coronavirus Morphogenesis

A. Viral Budding

Early electron microscopic studies demonstrated that coronavirus morphogenesis takes place at intracellular membranes and identified the cisternae of the endoplasmic reticulum as the site of budding of IBV and HCoV-229E (Becker *et al*., 1967; Chasey and Alexander, 1976; Hamre *et al*., 1967; Oshiro *et al*., 1971). Later studies revealed that early in infection particle formation occurs predominantly at smooth-walled, tubulovesicular membranes located intermediately between the rough endoplasmic reticulum and the Golgi complex (ERGIC). This so-called intermediate compartment was shown to be used as the early budding compartment by MHV, IBV, FIPV, TGEV, and SARS-CoV (Goldsmith *et al*., 2004; Klumperman *et al*., 1994; Tooze *et al*., 1984). At later times during infection the rough endoplasmic reticulum was seen to gradually become the major site of MHV budding in fibroblasts (Tooze *et al*., 1984).

As already mentioned, ultrastructural studies localized the MHV and IBV M proteins in the budding compartment(s) but also in the Golgi complex, that is, beyond the site of budding (Klumperman *et al*., 1994; Tooze *et al*., 1984). Apparently, accumulation of M protein alone

is not sufficient to determine the site of budding; other viral and/or cellular factors are required as well. For MHV the E protein, which was found to localize to the intermediate compartment by immuno-electron microscopy (immuno-EM), was suggested to be such a candidate (Raamsman *et al.*, 2000), but more players are likely to be involved. Whether the helical nucleocapsids, visible as electron-dense cytoplasmic elements adjacent to budding profiles (David-Ferreira and Manaker, 1965; Dubois-Dalcq *et al.*, 1982; Massalski *et al.*, 1982; Risco *et al.*, 1998; and references given previously), are a determining factor is unclear. In this respect, knowledge about the budding location of coronavirus-like particles (see later) might be informative.

B. Postassembly Maturation of Virions

Coronavirions are subject to an intracellular postbudding maturation process that occurs while they are on their way through the constitutive exocytic pathway by which they are exported out of the cell (Risco *et al.*, 1998; Salanueva *et al.*, 1999; Tooze *et al.*, 1987). Indications of this had already been noticed in early morphological studies with HCoV-229E (Becker *et al.*, 1967; Chasey and Alexander, 1976; Hamre *et al.*, 1967; Oshiro *et al.*, 1971) and MHV (Holmes and Behnke, 1981; Holmes *et al.*, 1981), but were described in somewhat more detail for MHV by Tooze and coworkers (1987). The pictures show "immature" virions in pre-Golgi compartments and Golgi cisternae that appear as spherical structures with the ribonucleoprotein core immediately below the viral envelope and with an "empty" center. By contrast, virions in the *trans*-Golgi network and beyond have the mature morphology showing a fairly uniform, high internal electron density.

An extensive analysis of the structural maturation of coronavirions was reported for TGEV (Risco *et al.*, 1998; Salanueva *et al.*, 1999). Budding was shown to yield relatively large virions with an annular, electron-dense internal periphery and a clear central area. Smaller particles, with the characteristic morphology of extracellular virions, that is, having a compact, dense inner core with polygonal contours, were seen to accumulate in secretory vesicles in the periphery of the infected cell. Both types of particles appeared to coexist in the Golgi complex (Fig. 5). Obviously, the larger particles are the precursors of the smaller mature virions (Salanueva *et al.*, 1999) and probably undergo their morphological maturation during their transport through the Golgi complex. The reorganization of the particle gives

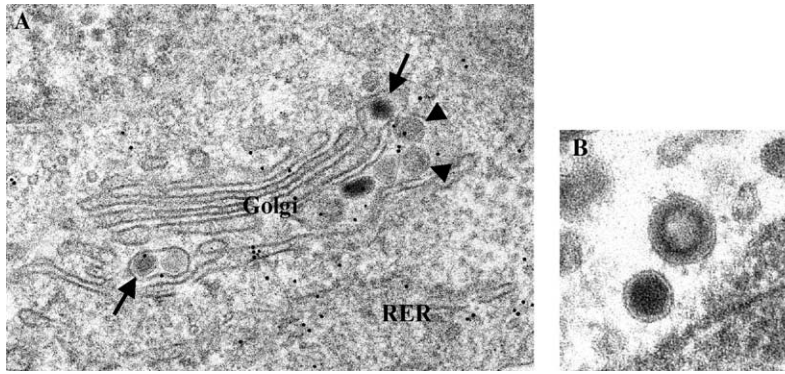

FIG 5. Structural maturation of coronavirus particles. Two types of virion-related particles were detected in TGEV-infected cells. Although large virions with an electron-dense internal periphery and a clear central area are abundant at perinuclear regions, smaller viral particles, with the characteristic morphology of extracellular virions, accumulate inside secretory vesicles that reach the plasma membrane. (A) Large virions (arrowheads) and small dense viral particles (arrows) coexist within the Golgi complex of infected cells (Risco *et al.*, 1998). (B) For a direct comparison of size and morphology a small, dense particle and a large particle are shown (Salanueva *et al.*, 1999). Pictures were kindly provided by C. Risco.

rise to the supposedly icosahedral core shell and is accompanied by a dramatic, approximately 50% reduction of the particle volume.

It is presently unknown what triggers the morphological reorganization in the Golgi complex. Application of drugs affecting the state of the organelle did not give clues. As virions encounter an increasingly acidic pH on passage through the Golgi stack, studies addressing this parameter were done with lysosomotropic agents. Thus, chloroquine and NH_4Cl were applied to MHV-infected cells to elevate the pH at the *trans* side of the Golgi complex, but no effect on the maturation of MHV was observed (Tooze *et al.*, 1987). Monensin, a drug that reversibly disorganizes the Golgi complex and blocks transport along the exocytic pathway, led to the accumulation of the large, annular TGEV virions; after reversal of the blockade formation of the small, compact particles was again restored (Salanueva *et al.*, 1999). These observations confirm that the Golgi complex is necessary for TGEV structural transformation. Nocodazole treatment of cells causes a reversible fragmentation of the Golgi complex. Under these conditions TGEV virions were still able to undergo normal structural maturation. In contrast, still another Golgi-disrupting compound, brefeldin A, prevented their maturation (Risco *et al.*, 1998). This compound leads

to a redistribution of Golgi membranes to the ER, leaving no definable Golgi system. Interestingly, MHV particles accumulated in infected cells under these conditions appeared to be infectious when liberated by sonication (J. Meertens and P. J. M. Rottier, unpublished results), leaving us with an intriguing question about the function of the maturation process.

IV. Molecular Interactions in Assembly of the Coronavirion

A. Nucleocapsid Assembly

1. Nucleocapsids in Infected Cells and Virions

Helical nucleocapsids are assembled in the cytoplasm of coronavirus-infected cells. They have been recognized by their tubular appearance in electron microscopy studies with several viruses including IBV, HCoV-229E, TGEV, and MHV (Becker *et al*., 1967; Chasey and Alexander, 1976; David-Ferreira and Manaker, 1965; Dubois-Dalcq *et al*., 1982; Hamre *et al*., 1967; Massalski *et al*., 1982; Oshiro *et al*., 1971; Risco *et al*., 1998). Large inclusions of nucleocapsids were seen to accumulate late in the infection of cells with HCoV (Caul and Egglestone, 1977) and MHV-JHM (Dubois-Dalcq *et al*., 1982).

The structure of the nucleocapsid as it occurs in infected cells has not been studied in any detail. Ribonucleoprotein particles supposed to represent nucleocapsids have been isolated from MHV-infected cells and were shown to consist of genomic RNA and N protein (Perlman *et al*., 1986; Robb and Bond, 1979; Spaan *et al*., 1981). The particles sedimented as EDTA-resistant structures of 200–230S in sucrose gradients. During the active phase of viral replication the majority (90%) of the intracellular genome-size RNA was found in these structures (Spaan *et al*., 1981).

Ultrastructural studies of nucleocapsids derived from purified virion preparations have shown quite a variety of helical structures, depending on the virus and the experimental conditions used. The overall feature, however, was that of a thread-like coil, sometimes appearing to be hollow, with a diameter varying between 9 and 16 nm and a length ranging from 0.32 μm up to 6 μm (Caul *et al*., 1979; Davies *et al*., 1981; Kennedy and Johnson-Lussenburg, 1975; Macnaughton and Davies, 1978)

Biochemical analysis of nucleocapsids prepared by detergent disruption of purified coronaviruses revealed the presence of genomic RNA and N protein. Interestingly, however, particles obtained by treatment

of virions with Nonidet P-40 appeared to be spherical when viewed under the electron microscope and, in addition, to contain M protein, as was observed with TGEV (Garwes *et al*., 1976), HEV (Pocock and Garwes, 1977), and MHV-JHM (Wege *et al*., 1979). The presence of the M protein was found for MHV-A59 to depend on the preparation conditions. Whereas the protein was absent when the virions had been disrupted with Nonidet P-40 at 4°C, solubilization at 37 °C resulted in copurification of M protein with the nucleocapsid (Sturman *et al*., 1980). The higher temperature was found to cause a conformational change in the M protein, leading to its aggregation and association with the viral RNA in the nucleocapsid. Similarly, nucleocapsid structures essentially lacking the M protein were also reported for IBV when virions were treated with detergent at low temperature (Davies *et al*., 1981).

Although there is no direct evidence yet, it seems reasonable to assume that the helical nucleocapsids seen accumulating in the cytosol of infected cells constitute the reservoir that feeds into the viral budding system. The location where these nucleocapsids are assembled has not been defined. Their production may take place either free in the cytoplasm, where the N protein is synthesized, or, alternatively, in association with the membrane-bound structures where genomic RNA is produced. The observed colocalization of N protein with the replication complexes (Bost *et al*., 2000, 2001; Denison *et al*., 1999; van der Meer *et al*., 1999) is consistent with the latter possibility. Coronavirus replication appears to occur on double-membrane vesicles (Gosert *et al*., 2002), which utilize components of the cellular autophagy pathway (Prentice *et al*., 2004). Whereas early in infection the replication complexes were shown to be almost entirely discrete from sites of M protein accumulation, at later times of infection helicase and N proteins appeared to colocalize with the M protein (Bost *et al*., 2000, 2001). It was proposed that the translocation of helicase–N protein complexes to sites of virus assembly may serve as a mechanism to deliver the newly synthesized RNA and nucleocapsids and to facilitate the retention of the M protein in the intermediate compartment.

2. Packaging Signals

Encapsidation of genomic RNA into a nucleocapsid is presumably initiated by an interaction of the N protein with a specific nucleotide sequence, the packaging signal, which is subsequently followed by the polymerization of N proteins around the RNA molecule in a non-sequence-specific manner. The selective incorporation of genomic RNA into virions would predict the packaging signal to be located in

sequences unique to this RNA, that is, within the approximately 20-kb region comprising the 5′ UTR and open reading frame 1 (ORF1) with the exception of the leader sequence. Although the data obtained so far support this prediction, no consistent picture has emerged yet.

The approach generally used to map the packaging signal involved the study of helper virus-assisted encapsidation of natural and artificially obtained defective RNA genomes. Thus, a 650-nucleotide region located at the 3′ end of the *pol1b* gene was initially identified for MHV (van der Most *et al.*, 1991), which was subsequently narrowed to an area of 190 nucleotides (Fosmire *et al.*, 1992). Within this area a stable stem–loop of 69 nucleotides was predicted. Mutation studies revealed that the integrity of this secondary structure was important and that the sequence of the packaging signal could be trimmed further to a minimum stretch of 61 nucleotides (Fosmire *et al.*, 1992). The signal appeared to be sufficient for RNA packaging as its inclusion allowed a synthetic subgenomic mRNA of MHV-A59 to be packaged specifically; the encapsidation efficiency of the mRNA was, however, significantly lower than that of the defective genomic RNA from which it was transcribed (Bos *et al.*, 1997). Even a nonviral RNA was found to be packaged into MHV particles when provided with the packaging signal (Woo *et al.*, 1997). Buoyant density analysis of the particles revealed that the RNA was not assembled separately but copackaged with helper virus RNA.

Studies of the corresponding *pol1b* region of another group 2 coronavirus, BCoV, indicated that within this group the packaging signal is structurally and functionally conserved. A 69-nucleotide sequence with significant homology (74%) to that of MHV was identified within a cloned 291-nucleotide segment sharing 72% homology overall (Cologna and Hogue, 2000). When this segment was fused to a noncoronavirus reporter gene sequence, the resulting RNA appeared to be packaged not only by the homologous helper virus BCoV but also by MHV. Conversely, when the MHV packaging signal was fused to the reporter gene sequence, the RNA was found to be encapsidated also in the context of a BCoV-infected cell (Cologna and Hogue, 2000).

Mapping studies of packaging signals in the genomes of group 1 and group 3 coronaviruses have yielded quite different results. For IBV, deletion mutagenesis of a defective RNA led to the conclusion that only the sequences in the 5′ UTR and/or a region of the 3′ UTR were specifically required for packaging, although parts of the *pol1b* sequence, but not any part in particular, also enhanced the efficiency (Dalton *et al.*, 2001). Somewhat similar conclusions could be drawn from a study with TGEV (Izeta *et al.*, 1999). By comparing packaging

efficiencies of different defective genomes it was inferred that information for packaging was present both at the genomic 5′ end (about 1.0 kb) and in parts of *pol1b*. A packaging signal was subsequently mapped to a fragment representing the 5′ terminal 649 nucleotides of the genome by inserting a series of overlapping segments covering a stretch of about 2300 nucleotides from the 5′ end of the genome into an mRNA reporter expression construct contained within a defective genome (Escors *et al*., 2003); only the 5′ terminal sequence conferred to the mRNA the ability to become packaged by helper virus.

It is too early to conclude that the apparently contrasting results reflect true, fundamental differences in encapsidation strategies between the different (groups of) coronaviruses. Although the overview may suggest the existence of different *cis*-acting signals, the data still allow a scenario in which multiple domains in the genome are involved cooperatively, each one contributing differently to (the efficiency of) the encapsidation process. Such contributions would not necessarily concern N protein binding only; the exceptional complexity of the coronaviral genome might call for additional provisions, related perhaps to the structuring of the encapsidation complex. Several observations indeed imply the involvement of multiple domains. The efficient rescue, for instance, of a BCoV defective genome (Drep) that completely lacks the putative 69-nucleotide packaging signal entails the participation of additional sequence(s) (Chang and Brian, 1996; Cologna and Hogue, 2000). Another example is the strongly increased rescue of an otherwise poorly packaged defective TGEV genome (M22) due to the presence of about 4.1 kb of sequences derived from the *pol1b* gene (M62) (Izeta *et al*., 1999).

3. N–RNA Interactions

There is no direct evidence yet for the actual functioning of the presumed packaging signals in the initiation of nucleocapsid assembly. Binding of N protein to these signals, the first step in the process, has so far been addressed only for the 69-nucleotide sequence of MHV. Specific binding to RNA transcripts containing this sequence was indeed demonstrated biochemically with MHV N protein derived from infected cells, from virions, and from cells expressing the protein (Molenkamp and Spaan, 1997). The binding efficiency, however, appeared to be relatively weak as was shown by comparing N protein binding to different parts of a packageable defective genome (MIDI-C) (Cologna *et al*., 2000). The highest binding efficiency was observed with an RNA transcript representing about 1 kb from the 5′ end of *pol1a*. Remarkably, not even removal of the packaging signal from

MIDI-C RNA affected binding to the N protein as measured in the filter-binding assay used. The observations indicate that the domain containing the 69-nucleotide sequence does not function as a packaging signal in the conventional sense, adding further support to the notion that the intricacies of coronaviral nucleocapsid assembly are complex.

Apart from the studies mentioned, the occurrence of N–RNA interactions has been amply documented. This is not surprising as the N protein has been implicated in several other processes that involve interaction with RNA, such as replication, transcription, and translation (Lai and Cavanagh, 1997; see also Section II.C). As the relevance of these interactions for viral assembly is generally unclear, a brief survey of the available information is included here. In addition, an overview of data on the mapping of RNA interactions on the N polypeptide is schematically presented in Fig. 6.

A high-affinity interaction between the N protein and the 5′ leader was demonstrated for MHV-A59 (Stohlman *et al.*, 1988). Using an RNA overlay protein blot assay and various *in vitro* RNA transcripts, the binding of N protein was localized to a stretch of nucleotides (nucleotides 56–65) at the 3′ end of the leader (Stohlman *et al.*, 1988). The stretch included the pentanucleotide repeat UCUAA now known to be critical for transcription. Biochemical analyses of the interaction measured a dissociation constant (K_d) of 14 nM for bacterially expressed MHV N protein to the leader RNA (Nelson *et al.*, 2000). Consistent with the presence of a leader at the 5′ end of all viral RNAs, an N protein-specific monoclonal antibody coimmunoprecipitated genomic RNA as well as the subgenomic RNAs from MHV-infected cells (Baric *et al.*, 1988). Similar observations were made for BCoV (Cologna *et al.*, 2000). Packaging of subgenomic RNAs has been reported for TGEV (Sethna *et al.*, 1991), BCoV (Hofmann *et al.*, 1990), and IBV (Zhao *et al.*, 1993) but not for MHV, suggesting that their incorporation is not mediated by N protein–leader interaction. Whereas for TGEV and IBV the relative packaging of subgenomic RNAs was found to be inefficient, genomic RNA appearing in virions at a more than 10-fold molar excess over any subgenomic RNA species, the BCoV subgenomic N and M mRNAs appeared to be packaged as abundantly as the genome (Hofmann *et al.*, 1990). A reevaluation for TGEV revealed that the detection of subgenomic RNAs in virions was related to the purity of virus preparations, indicating that mRNAs were not specifically encapsidated (Escors *et al.*, 2003).

Besides the leader, the N protein has been found to bind to other parts of the coronaviral genome. In addition to the binding site in the MHV

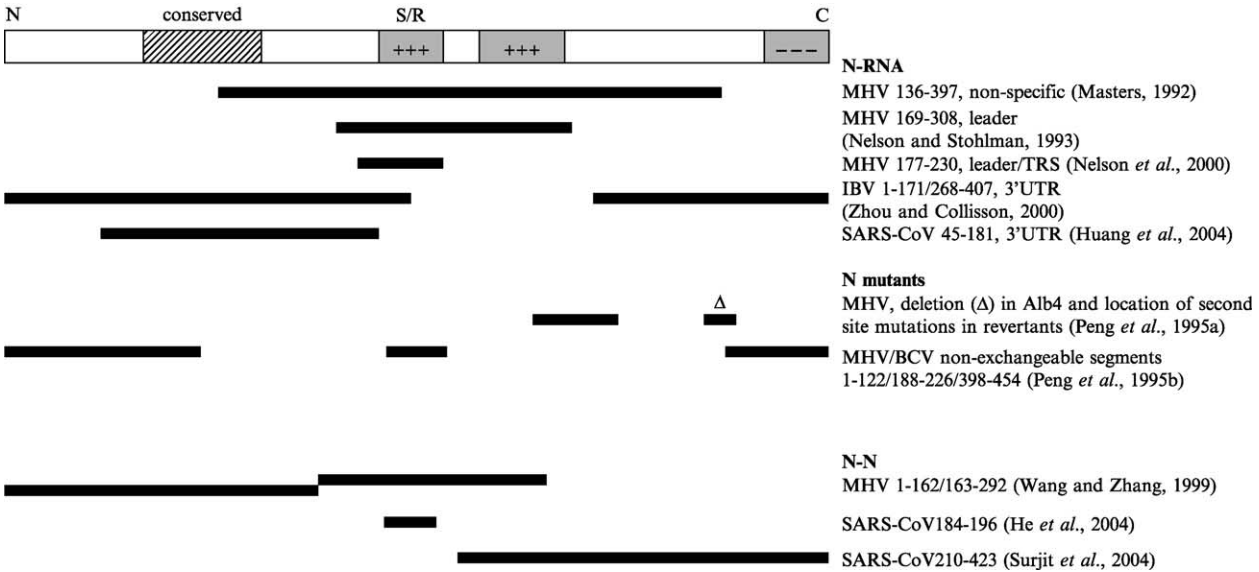

FIG 6. Structural organization of the coronavirus N protein. Common features and their distribution along the polypeptide chain are shown schematically. The hatched box indicates the most conserved part of the N protein, with a high proportion of aromatic residues. The N protein contains many basic residues throughout the polypeptide, but with particular clustering in two regions (+++). The upstream cluster contains a serine/arginine-rich region (S/R). The carboxy terminus, which contains a high proportion of acidic residues, is also indicated (– – –). The bars indicate parts of the N protein that have been implicated in N–N and N–RNA interaction. Furthermore, the location of the deletion in the MHV-A59 mutant Alb4 (Δ) is indicated as well as the domain where second-site mutations in revertant viruses of Alb4 are mapped. Finally, the parts of the N protein that could not be transferred from BCV into the MHV genome are marked. References are included in the figure.

pol1a gene mentioned previously, a high-efficiency binding site was identified by the same authors in the 3′ half of the N gene of both MHV and BCoV (Cologna *et al.*, 2000). The IBV N protein was shown to bind sequences in the 3′ terminal UTR of the genome (Zhou *et al.*, 1996).

Coronavirus N proteins do not contain sequence motifs typically found in other RNA-binding proteins. They appear to bind RNA both nonspecifically (Masters, 1992; Robbins *et al.*, 1986) and in a sequence-specific way (Cologna *et al.*, 2000; Nelson and Stohlman, 1993; Nelson *et al.*, 2000; Stohlman *et al.*, 1992). Non-sequence-specific RNA binding has been mapped to a large central domain of the MHV N molecule (Fig. 6) (Masters, 1992). Also, the leader-binding property was assigned to this domain; this activity was initially mapped to the area containing the two highly basic regions (Nelson and Stohlman, 1993), but was later narrowed to a 55-residue segment containing the serine/arginine-rich basic region (Nelson *et al.*, 2000). Interestingly, this particular region could not be interchanged with its BCoV counterpart in a study on the functional equivalence of the N proteins from these related viruses (Peng *et al.*, 1995b). Another domain in the MHV N protein implicated in viral RNA binding was mapped to an area that partly overlaps with the second basic region. The assignment was based on an analysis of second-site revertants of MHV mutant Alb4, the virions of which are extremely thermolabile because of a 29-residue deletion located between the central and carboxy-terminal domain of the N protein (Koetzner *et al.*, 1992). The reverting mutations correlated with restoration of the disturbed RNA-binding capacity of the MHV N protein and were found clustered close to the basic region some 80 residues on the amino side of the deletion (Fig. 6) (Peng *et al.*, 1995a). Although all these studies consistently attribute a major role in RNA binding to the central portion of the coronaviral N protein, the interaction of the IBV N protein with the 3′ UTR of IBV RNA mentioned previously was mapped to the amino- and carboxy-terminal domains of the molecule (Zhou and Collisson, 2000). 3′ UTR RNA-binding activity was also assigned to the amino-terminal domain of the SARS-CoV N protein on the basis of studies using nuclear magnetic resonance spectroscopy (Huang *et al.*, 2004).

4. N–N Interactions

It is obvious that the wrapping of the 30-kb coronaviral genome into the compact helical nucleocapsid is largely driven by N protein interactions. As there are no indications for packaging of the RNA into a preformed capsid, these interactions can be described by the following model. Packaging is initiated by binding of the N protein, either

as a monomer or in a multimeric form, to the RNA. By analogy to other RNA viruses, this sequence-specific interaction may induce a conformational change in the N protein, thereby creating a nucleation site for the cooperative stacking of N protein units along the entire length of the RNA, now in a non-sequence-specific way. These N units can again be monomeric or consist of defined multimers. Finally, helix formation is driven by interactions between N molecules separated along the ribonucleoprotein chain but that become adjacent in neighboring helices. This model predicts multiple nonequivalent interactions between N molecules.

N–N interactions have been experimentally demonstrated for MHV, BCoV, and HCoV-OC43. High molecular weight species of the N protein, possibly trimers, were detected by sodium dodecyl sulfate–polyacrylamide gel electrophoresis (SDS–PAGE) of virion preparations under nonreducing (but not under reducing) conditions, which is indicative of intermolecular disulfide bonds between the N subunits (Hogue *et al*., 1984; Narayanan *et al*., 2003b; Robbins *et al*., 1986). These complexes are likely to be additionally stabilized by noncovalent interactions as coronavirus N protein cysteines are not well conserved, the SARS-CoV N protein even lacking any cysteine residues. Both monomeric and oligomeric N species were able to bind RNA (Robbins *et al*., 1986). Multimeric forms of the N protein were also found in association with intracellular genomic RNA in MHV-infected cells as shown after the selective isolation of this ribonucleoprotein through coimmunoprecipitation with the M protein (Narayanan *et al*., 2003b). High molecular weight forms of the N protein corresponding to dimers and trimers were also demonstrated *in vitro* after ultraviolet (UV) cross-linking of BCoV N protein to RNAs (Cologna *et al*., 2000).

Few studies have addressed the identification of the N–N interaction domains. The results so far are inconsistent (Fig. 6), but this might as well reflect the predicted occurrence of nonequivalent interactions. Interaction sites were mapped to the amino-terminal part of the MHV N protein (Wang and Zhang, 1999). Using an *in vitro* binding assay in which the full-length N protein was incubated with bacterially expressed fusion proteins containing different segments of the N protein, interaction was observed with a polypeptide derived from the amino-terminal one-third (residues 1–162) of the protein and with a polypeptide representing the central part (residues 163–292). The latter domain contains the serine/arginine-rich region implicated in the binding to the leader/TRS-specific sequences (Nelson *et al*., 2000). This domain could not be replaced by the corresponding domain from BCoV without loss of viral viability, from which the authors

indeed inferred an involvement in protein–protein interactions (Peng *et al.*, 1995b). The same domain was also shown to be essential for the homotypic association of the SARS-CoV N protein (He *et al.*, 2004). Using a mammalian two-hybrid approach, the N–N interaction appeared to be abolished completely when the serine/arginine-rich region had been deleted. However, in another study using the yeast two-hybrid system this interaction was not confirmed. A polypeptide consisting of the amino-terminal two-thirds of the SARS-CoV N protein, that contains the serine/arginine-rich region, exhibited no association with the full-length protein (Surjit *et al.*, 2004). Rather, self-association was attributed to the carboxy-terminal 209 residues of the molecule, which lacks the motif.

B. Envelope Assembly

1. Formation of Virus-Like Particles: M–E Interactions

Unlike most other enveloped viruses, coronaviruses have the remarkable feature of being able to independently assemble their envelope. Indications for this were already noticed in early electron microscopy studies of viral preparations and infected cells showing the occurrence of apparently "empty" particles (Afzelius, 1994; Chasey and Alexander, 1976; Macnaughton and Davies, 1980). Incomplete virions with the typical coronavirus morphology but lacking the N protein and the genome could indeed be separated from normal IBV particles by their lower density in sucrose gradients (Macnaughton and Davies, 1980). The definition of virus-like particles (VLPs) and the requirements for their formation were established by the coexpression of the coronaviral structural proteins in mammalian cells (Vennema *et al.*, 1996). Membranous particles were assembled when the MHV envelope proteins M, E, and S were coexpressed, without the need for an N protein or genomic RNA. The particles were released from the cells and, when examined under the electron microscope, appeared to be morphologically indistinguishable from authentic virions, that is, they had the characteristic shape and dimensions of normal virions. Also, their membrane protein composition was similar to that of MHV, with a high abundance of M protein and only trace amounts of E protein. Quite surprisingly, only the M and E proteins were required for particle assembly. Both S and N proteins were dispensable for particle formation but, whereas the S protein became incorporated when present, this was not the case for the N protein (Vennema *et al.*, 1996), except in combination with (defective) genomic RNA, in which case a

nucleocapsid was coassembled (Bos *et al*., 1996; Kim *et al*., 1997). Individual expression of the M or the E protein in cells did not give rise to formation of VLPs although E protein synthesis by itself led to the secretion of E-containing vesicles (Corse and Machamer, 2000; Maeda *et al*., 1999). The nature of these particles has not been characterized in much detail; the vesicles induced by MHV E sedimented slightly slower than virions (Maeda *et al*., 1999) whereas the particles obtained with IBV E had about the same density as virions (Corse and Machamer, 2000).

Besides for MHV and IBV, VLPs have so far been described for BCoV (Baudoux *et al*., 1998b), FIPV (Godeke *et al*., 2000), and TGEV (Baudoux *et al*., 1998b). The observations demonstrate the unique budding mechanism of coronaviruses, which is dependent solely on the envelope proteins M and E but independent of a nucleocapsid. Somewhat similar observations have been described for the flavivirus tick-borne encephalitis virus and for hepatitis B virus, which also produce proteolipid particles on expression of their envelope proteins preM and E (Allison *et al*., 1995; Mason *et al*., 1991) and S (Patzer *et al*., 1986; Simon *et al*., 1988), respectively, but these particles are much smaller than the corresponding virions. In contrast, particles with the typical, large size of coronaviruses are acquired by the concerted action of just the proteins M and E (Baudoux *et al*., 1998b; Vennema *et al*., 1996). Budding of enveloped viruses generally requires a nucleocapsid (for a review see Garoff *et al*., 1998). For retroviruses the Gag protein, the precursor to the nucleocapsid, is all that is needed to obtain particles resembling immature virions; the Env protein is dispensable. Budding of alphaviruses, on the other hand, requires both the envelope proteins and the nucleocapsid. Interestingly, the same appears to hold true for arteriviruses (R. Wieringa, A. A. F. de Vries, and P. J. M. Rottier, unpublished observations), which are closely related to the coronaviruses, share with them a triple-spanning envelope protein, and bud into early membranes of the secretory pathway, like coronaviruses but unlike alphaviruses.

It is unknown how the coronavirus M and E proteins cooperate in budding. As the extensive electron microscopy work with M proteins from various coronaviruses gave no indications that this protein causes membrane bulging by itself, it is believed that the function of the E protein in coronavirus budding is in the induction of curvature in the M protein lattice (see later) and the subsequent budding of the membrane (Vennema *et al*., 1996). By its low abundance in the virion, the E protein does not seem to serve a genuine structural function in that it occupies frequent, regular positions in the M protein framework. Consistent

with an important role of the E protein in particle morphogenesis, mutations in its hydrophilic carboxy-terminal part, introduced by targeted recombination into the MHV genome, yielded thermolabile viruses one of which showed aberrant virion morphology with pinched and elongated shapes when viewed in the electron microscope (Fischer *et al.*, 1998). Revertant analyses revealed that a single second-site amino acid change within the E protein was able to reverse the phenotypic effect of the original mutations, providing support for possible interactions between E protein monomers during budding (Fischer *et al.*, 1998). Unexpectedly, complete deletion of the E gene from the coronaviral genome does not abolish virion formation, demonstrating that the protein is not essential for budding. Whereas this deletion dramatically (at least 1000-fold) reduced the release of infectivity from infected cells in the case of MHV-A59 (Kuo and Masters, 2003), knockout of the TGEV E gene resulted in a lethal phenotype (Curtis *et al.*, 2002; Ortego *et al.*, 2002). Remarkably, however, in the latter case virions still assembled but these appeared to be unable to leave the cells (J. Ortego and L. Enjuanes, personal communication).

The VLP system offers a convenient assay to study many aspects of coronavirus envelope assembly. It was thus used to analyze the primary structure requirements of the M and E proteins for particle formation. For the M protein such studies demonstrated each of its different domains to be important. In general, mutations (deletions, insertions, and point mutations) in the lumenal domain, the transmembrane domains, the amphiphilic domain, or the carboxy-terminal domain of the MHV M protein strongly affected its ability to form VLPs (de Haan *et al.*, 1998a). The assembly process was particularly sensitive to changes in the carboxy terminus of the protein. Truncation by only one residue reduced the efficiency severely whereas removal of two residues fully abolished particle formation. These effects appeared to be less severe in the context of a normal coronaviral infection, probably because additional interactions can compensate. The single-residue deletion, when introduced into the MHV genome, was without measurable phenotype and also a mutant virus with a truncation of two residues could be obtained, although with difficulty, as it was severely affected in its growth (de Haan *et al.*, 1998a; Kuo and Masters, 2002). The importance of the M protein cytoplasmic and transmembrane domains was confirmed by VLP studies in the IBV system; mutant proteins lacking portions of either of these domains were unable to support particle assembly (Corse and Machamer, 2003).

Studies of the primary structure requirements of the E protein for VLP formation revealed that the sequence of its hydrophobic domain

was not critical. The assembly capacity of the protein was maintained when its transmembrane region was partly or completely replaced by the corresponding domain of the vesicular stomatitis virus (VSV) G protein (Corse and Machamer, 2003). However, when its small amino-terminal ectodomain was additionally replaced by the large VSV G protein counterpart, the chimeric protein became nonfunctional. Deletion of the transmembrane, but not the amino-terminal, domain rendered the E protein essentially assembly incompetent (Lim and Liu, 2001). Deletions in the cytoplasmic carboxy-terminal half of the E protein mapped the cysteine-rich region as the most important part for VLP assembly (Lim and Liu, 2001).

Although the interaction between M and E proteins is amply demonstrated by their interdependence for VLP formation, direct evidence for their interaction has actually been provided only for the IBV proteins (Corse and Machamer, 2003; Lim and Liu, 2001). The two proteins could be cross-linked to each other in IBV-infected cells and in cells coexpressing the M and E genes (Corse and Machamer, 2003). It appeared that the cytoplasmic tails of both proteins were required, suggesting they are involved in the interaction. In another study M–E interaction was demonstrated by a coimmunoprecipitation assay. Also in this assay the cytoplasmic domain of the E protein, comprising the cysteine-rich region, was found to be important as its deletion affected M–E interaction to the greatest extent when compared with other deletion mutant E proteins (Lim and Liu, 2001). The results from both studies also showed that the ability of mutant E or M proteins to interact did not correlate with their assembly competence. Apparently, other requirements such as homotypic E or M interactions or interactions with host cell components must be met.

The specificity of the interaction between the M and E proteins during particle assembly was further demonstrated by the poorly successful attempts to generate chimeric VLPs. No particles were observed when heterologous combinations of TGEV and BCoV M and E proteins were coexpressed (Baudoux *et al.*, 1998b) and the same was true for heterologous combinations of FIPV and MHV M and E proteins (H. Vennema and P. J. M. Rottier, unpublished results). In both studies chimeric M and E proteins were also tested, demonstrating that, except in one case, exchanges between corresponding domains rendered the proteins assembly incompetent. Only when the TGEV M protein amino-terminal ectodomain was replaced with that of BCoV did the chimeric polypeptide support VLP formation in combination with the TGEV E protein; VLP formations was also supported, but to different extents, with TGEV/BCoV chimeric E proteins and—poorly,

however—with the BCoV E protein (Baudoux *et al*., 1998b). The reciprocal M construct, the BCoV M protein carrying the TGEV ectodomain, was nonfunctional, even in combination with TGEV E protein. Consistently, replacement of the ectodomain with that of FIPV M also abolished the productive partnership of MHV M protein with MHV E (de Haan *et al*., 1999).

2. M–M Interactions

As the disproportionate amounts of M and E proteins in VLPs already imply, homotypic interactions between M molecules must constitute the energetic basis underlying the formation of the coronaviral envelope. In MHV-based VLPs generated by coexpression of M and E proteins, for instance, the sheer excess of M protein—the relative molar presence of E in the particles is less than 1%—is evidence for the strong interactive forces between M molecules. Hence, envelope assembly is thought to be driven primarily by laterally interacting M molecules that form a two-dimensional lattice in intracellular membranes (Opstelten *et al*., 1993b, 1995). Large multimeric complexes of M protein have indeed been demonstrated biochemically after individual expression of the MHV protein in cells. When the association of the M molecules was maintained by the careful selection of cell lysis conditions, sucrose gradient analysis revealed the existence of large heterogeneous (up to about 40 molecules) complexes, which accumulated in the Golgi compartment (Locker *et al*., 1995). Somewhat smaller complexes were obtained when the cytoplasmic tail of the protein was removed; these complexes were no longer retained in the Golgi apparatus but transported to the cell surface. Apparently, the tail domain is not essential for the lateral interactions between M proteins, but it is critically required for budding (de Haan *et al*., 1998a, 2000). Similar higher order complexes of the M protein have also been demonstrated in MHV-infected cells as well as in MHV virions (Opstelten *et al*., 1993b, 1995).

Further support for the existence of homotypic M protein interactions and additional insight into the domains involved in these interactions came from work with mutant M proteins that are unable to assemble into VLPs. In these studies MHV M proteins with deletions in either the transmembrane regions, the amphipathic domain, or the extreme carboxy terminus or with substitutions of the lumenal domain were tested for their ability to associate with other M proteins and to be rescued into VLPs formed by assembly-competent M proteins (de Haan *et al*., 1998a, 2000). It appeared that the mutant proteins maintained these biological activities despite the often severe

alterations; actually, the only mutant protein that had lost these abilities was one in which all three transmembrane domains had been replaced by a heterologous transmembrane domain. It was concluded that M protein molecules interact with each other through multiple contact sites, particularly at the transmembrane level. It was furthermore hypothesized that the full complement of interactions between the M molecules is required for efficient particle formation; possibly, all these interactions are required to provide the free energy to generate and stabilize the budding envelope. The failure of M protein mutants capable of associating with assembly-competent M protein to assemble into VLPs by themselves (de Haan *et al*., 1998a, 2000) indicates that additional interactions with viral (E) and/or host proteins is required. In this respect it is of note that the IFN-inducing capacity of the M protein, demonstrated for TGEV and BCoV, also requires the presence of the E protein, which suggests that the induction of IFN is dependent on a specific, probably regularly organized structure of the M protein (Baudoux *et al*., 1998a,b). It is unclear how the presence of the E protein alters the M protein lattice to achieve this effect.

3. M–S and M–HE Interactions

Coronavirus envelope assembly is not dependent on the S protein or the HE protein. This is obvious from work with VLPs as well as with viruses showing that bona fide particles were produced when these proteins were either simply absent or unavailable for assembly. Availability can be compromised under conditions in which proper folding of the proteins is affected. Inhibition of N-glycosylation by the drug tunicamycin, for instance, can lead to aggregation and retention of membrane proteins in the endoplasmic reticulum and has been shown to prevent the incorporation into virions of both the S protein (Holmes *et al*., 1981; Mounir and Talbot, 1992; Rottier *et al*., 1981a; Stern and Sefton, 1982) and the HE protein (Mounir and Talbot, 1992). The same effect has been observed with temperature-sensitive MHV mutants carrying defects in their S gene, which, when grown at the restrictive temperature, gave rise to spikeless particles (Luytjes *et al*., 1997; Ricard *et al*., 1995).

Both S and HE proteins are assembled into the coronaviral envelope through interactions with the M protein. Such interactions have been demonstrated for MHV and BCoV M and S proteins and for BCoV M and HE proteins, in infected cells, in cells coexpressing the proteins, and in virions (Nguyen and Hogue, 1997; Opstelten *et al*., 1995). Complexes of the proteins were shown by coimmunoprecipitation and cosedimentation analyses as well as by immunofluorescence studies

in which the intracellular transport of S and HE proteins to the plasma membrane was found to be inhibited by coexpressed M protein, the proteins being retained in the Golgi apparatus, the natural residence of the M protein.

The kinetics with which the proteins engage in heteromeric complex formation appeared to be different for the different proteins. This effect is due to their different rates of folding and oligomerization. For the S protein these rates are low, involving the formation of multiple intramolecular disulfide bonds and the addition of numerous oligosaccharide side chains (Delmas and Laude, 1990; Opstelten *et al*., 1993a; Vennema *et al*., 1990a,b). In contrast, folding of the MHV and BCoV M proteins is independent of disulfide bonds and glycosylation, as a result of which they are, for instance, swiftly transported out of the endoplasmic reticulum (Opstelten *et al*., 1993a). As a consequence, M molecules enter into M–S and M–HE complexes immediately after their synthesis whereas for newly synthesized S and HE molecules it took 15-30 min before they started to appear in these heterocomplexes (Nguyen and Hogue, 1997; Opstelten *et al*., 1995). The importance of folding as a major rate-limiting step was illustrated by the inability of the S protein to interact with M protein when its folding had been inhibited by *in vivo* reduction; only completely oxidized S molecules were association competent (Opstelten *et al*., 1993a, 1995). Whether the M protein interacts with S and HE proteins while they are still in their monomeric form or only after their oligomerization remains to be elucidated. It is, however, clear that the proteins engage in interaction with each other in early compartments, most likely the endoplasmic reticulum, as judged from the oligosaccharide maturation states of freshly formed protein complexes (de Haan *et al*., 1999; Nguyen and Hogue, 1997; Opstelten *et al*., 1995). Only dimers of HE were associated with HE–M–S complexes that were observed in BCoV-infected cells; because the appearance of HE in these complexes correlated with the kinetics of HE dimerization it was concluded that proper oligomerization is most likely a requirement for its association (Nguyen and Hogue, 1997). Interestingly, such heterotrimeric complexes were not observed on coexpression of the three proteins in cells. Under these conditions only the heterodimeric M–S and M–HE associations were detected.

The structural domains of M and S proteins that are involved in the formation and stabilization of their complex have been identified. Using the coimmunoprecipitation and colocalization assays referred to previously, the essential domains in the MHV M protein were mapped by a mutagenetic approach (de Haan *et al*., 1999). It appeared that M–S complex formation was sensitive to changes in all membrane-

associated parts of the M molecule. Interactions between M and S proteins were found to occur at the level of the transmembrane domains and of the amphipathic domain, which is located on the cytoplasmic face of cellular membranes. In contrast, neither the lumenally exposed amino terminus nor the hydrophilic cytoplasmic tail of the M protein was required; even the deletion of these parts—known to abrogate the ability of the protein to form VLPs—did not prevent association with the S protein.

Chimeric S proteins were used to show that the large ectodomains of the spikes are not involved in interaction with M proteins. Such chimeric proteins were constructed from the MHV and FIPV S proteins and consisted of the ecto- or lumenal domain from the one and the transmembrane plus endodomain from the other. These proteins, which seemed biologically fit as they were still fusion active, were initially tested in coexpression studies with the M and E proteins from either virus for their ability to be incorporated into VLPs. They were found to assemble only into viral particles of the species from which their carboxy-terminal domain originated (Godeke *et al.*, 2000). The chimeric S genes were subsequently incorporated into the proper coronavirus genomic background, creating the chimeric viruses fMHV and mFIPV, the spike ectodomains of which are from the feline and murine coronavirus, respectively; these studies provided the basis for the development of a novel targeted recombination system for reverse genetics of coronaviruses (Haijema *et al.*, 2003; Kuo *et al.*, 2000).

Further fine mapping of the carboxy-terminal parts of the S protein involved in M–S protein interaction revealed the importance of the cytoplasmic tail. Again using coimmunoprecipitation and VLP incorporation assays, it appeared that increasing truncations gradually abolished the association with the M protein (B. J. Bosch, C. A. M. de Haan, and P. J. M. Rottier, unpublished results). The significance of the tail domain was demonstrated most convincingly by showing the coimmunoprecipitation and VLP assembly of a chimeric VSV G protein the cytoplasmic tail of which had been replaced by that of MHV S. Tail truncations were tolerated in the context of the coronavirus; recombinant MHVs were generated that lacked 12 or 25 (but not 35) residues from the S protein carboxy terminus, but their growth was impaired by about 10- and 10^4-fold, respectively. Also, tail extensions were tolerated, allowing the construction of a recombinant MHV with a spike protein extended at its carboxy terminus by the green fluorescent protein (GFP), yielding green fluorescent virions (Bosch *et al.*, 2004a). The extension was, however, lost quite rapidly on serial passaging of the virus.

Molecular details of the interaction of M and HE proteins and the requirements of HE for incorporation into viral particles have not been described. One study reported that HE protein mutants lacking part of their ectodomain were not assembled into particles (Liao *et al.*, 1995). Most likely, however, this observation was due to folding or maturation defects of the mutant proteins. In another study the BCoV S and HE proteins were shown to be incorporated into MHV particles when coexpressed in MHV-infected cells. Apparently, homology between the proteins of these related group 2 coronaviruses is sufficiently high for heterologous M–S and M–HE interactions to occur (Popova and Zhang, 2002).

C. Virion Assembly

1. Envelope–Nucleocapsid Interactions

Numerous electron microscopy studies have pictured the process of virion assembly in the coronavirus-infected cell. They show the close apposition of—presumably preassembled—tubular nucleocapsids to intracellular membranes, the appearance of membrane curvature at the contact sites, the "growth" of these buds into particle-sized vesicles, and the ultimate detachment of virions from the membranes by pinching off.

It has become clear that the M protein is the central player, which, through its interactions with every known component of the virion, orchestrates the entire assembly process (see Fig. 7). In the process two levels of interaction can be distinguished. One is the level of the membrane where, as detailed in the previous section, the M protein interacts (1) with itself, to generate the basic molecular framework of the viral envelope, (2) with the E protein, to induce curving and budding of the M protein-modified membrane, and (3) with S and HE, to coassemble these spikes into the viral envelope. The other level at which the M protein operates involves the incorporation of the nucleocapsid into the virion. Here, two types of interactions have been described: interactions of the M protein with the N protein and with the viral genome.

An instrumental role of the M protein in drawing the nucleocapsid into the budding particle is indicated by their demonstrated interaction in studies with virion preparations. The M protein has been shown to remain associated with subviral particles obtained after treatment of virions with detergent that removes the spikes (Escors *et al.*, 2001a,b; Garwes *et al.*, 1976; Lancer and Howard, 1980; Wege *et al.*, 1979).

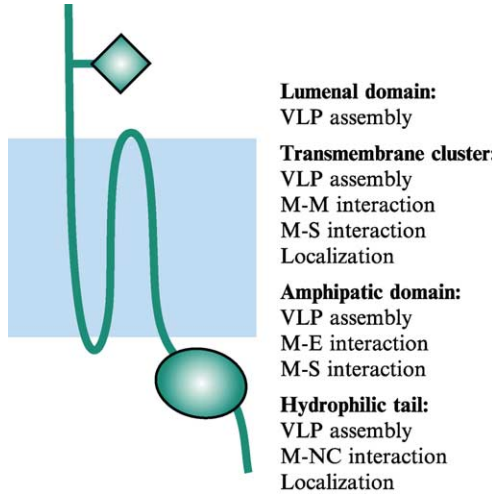

FIG 7. The various domains of the MHV M protein and the processes for which they are important. The amphipathic domain of the M protein is represented by an oval. See text for references.

The association was shown for MHV to be temperature dependent (Sturman *et al*., 1980). In the case of TGEV the association of M with the spherical structure, termed the core, was stabilized by basic pH and divalent cations but lost at high salt concentration, resulting in disruption of the core structure and release of the helical nucleocapsid (Escors *et al*., 2001a,b; Risco *et al*., 1996). In an elegant study of the binding of *in vitro*-translated M polypeptides to purified nucleocapsids the ionic interaction was mapped to a 16-residue sequence in the hydrophilic carboxy-terminal tail domain (Escors *et al*., 2001b). Also in infected cells, interaction of the M protein with ribonucleoprotein structures, presumably nucleocapsids, has been demonstrated. Using M-specific antibodies, structures containing both N protein and genomic RNA were coimmunoprecipitated with M protein from MHV-infected cell lysates (Narayanan *et al*., 2000). Conversely, M protein was coprecipitated when an N-specific antibody was used, while in this case all viral mRNAs copurified because of their known leader-mediated affinity for the N protein. These interactions did not require an S or an E protein (Narayanan *et al*., 2000).

Although interactions between the M and N proteins might intuitively be expected to drive the process of attachment of the nucleocapsid to the intracellular target membrane, direct experimental evidence

for this interaction is strikingly lacking. Significantly, MHV M and N proteins coexpressed in cells were found not to interact (Narayanan *et al.*, 2000) nor did purified TGEV N protein interact with *in vitro*-synthesized M protein (Escors *et al.*, 2001b). Because the N protein occurs in coronavirus-infected cells in various configurations—as a free protein and in association with an array of partners including the viral genome—it is obvious that a selection mechanism must act to ensure that only nucleocapsids are assembled into particles. Consistently, coexpressed N protein is not incorporated into VLPs, but its inclusion depends on the presence of viral RNA (Bos *et al.*, 1996; Vennema *et al.*, 1996). Thus, unless the selection process is performed by a mechanism not involving the N protein, its association with genomic RNA to form a nucleocapsid seems required to generate the unique conformation that enables it to interact with the M protein. The only evidence to date for an interaction between M and N proteins is indirect and comes from genetic studies. Analysis of second-site revertants of a constructed MHV-A59 mutant virus lacking the two carboxy-terminal residues of its M protein revealed that the highly defective growth phenotype of this virus could be restored, among others, by mutations in the carboxy-terminal domain of the N protein (Kuo and Masters, 2002). In two independently obtained revertants the N protein had lost 15 residues of this—among different strains of MHV highly conserved—domain because of a frameshifting 10-nucleotide deletion. The results argue strongly for a direct cooperation of the carboxy-terminal regions of the M and N proteins during virion formation. Other indications supporting the occurrence of M–N interactions come from studies of complexes of M protein with ribonucleoprotein from MHV-infected cells and with TGEV cores (Escors *et al.*, 2001b; Narayanan *et al.*, 2000). When such complexes were treated with RNase the association of M and N proteins was not destroyed, suggesting a direct interaction. However, the presence of short RNAs inaccessible to the RNase but sufficient to bridge the M–N interaction could not be excluded.

The most unusual interaction that the coronaviral M protein seems to engage in involves genomic RNA. This interaction has so far been reported only for MHV, by Makino and co-workers. These workers had shown earlier that the 69-nucleotide packaging signal located in the *pol1b* gene could mediate the incorporation into virions of RNAs of even noncoronaviral origin (Woo *et al.*, 1997). They subsequently showed that this incorporation is most likely effected by a direct and specific interaction of the signal with the M protein. When defective genomic RNAs or nonviral RNAs were introduced into helper MHV-

infected cells, they could subsequently be isolated as ribonucleoproteins from lysates of the cells by immunoprecipitation with an M-specific antibody, but only if the RNAs contained the packaging signal (Narayanan and Makino, 2001). Coexpression experiments using noncoronaviral vectors showed the interaction to be independent of the N protein. A reporter gene transcript generated in cells expressing the M protein could be coimmunoprecipitated with an anti-M monoclonal antibody provided that the RNA carried the packaging signal (Narayanan *et al*., 2003a). Moreover, when the E protein was additionally coexpressed, the signal-containing RNA—but not an identical RNA lacking this sequence—was found to be coincorporated into VLPs, irrespective of the presence of the N protein. Altogether these observations reveal a hitherto unknown type of interaction between a viral envelope protein and genomic RNA. Although its significance remains to be further established the M–RNA interaction seems to provide additional selectivity to the assembly of the coronaviral nucleocapsid.

2. *Specificity and Flexibility*

Assembly of viruses is a process of generally high specificity. Directed by specific targeting signals, the viral structural components colocalize to distinct places in the cell where unique and complex molecular interactions control their assembly. These rules hold particularly for naked viruses and many of the smaller enveloped viruses; there are, however, many examples where the process is considerably less selective and where "nonself" (host or viral) components are coassembled (see, e.g., Garoff *et al*., 1998). Interestingly, formation of the large, pleiomorphic coronaviruses appears to combine aspects of both great selectivity and extreme flexibility.

With the M and E proteins as the fixed minimal requirement, coronaviral particles appear to tolerate the presence of all other viral components in practically every possible combination. A nucleocapsid is not required but, if available, it can take almost any length as defective (including chimeric) genomes of largely varying sizes have been accommodated. RNAs need not necessarily be packaged into a nucleocapsid; whether of viral or nonviral origin, if provided with the proper packaging signal they can be taken in even in the absence of an N protein.

Also in the composition of their viral envelope these viruses are highly flexible. Spikes seem to be incorporated in variable numbers depending on availability. They tolerate severe manipulation, both of their ectodomain and of their endodomain. Thus, swapping of ectodomains between unrelated coronaviruses (i.e., from different groups)

creates viable chimeric viruses whereas a foreign protein such as GFP appended to the S protein endodomain is accommodated in the particle, although reluctantly. Some coronaviruses have an HE protein but continue growing well if for any reason the gene is not (properly) expressed as happens among different MHVs. Consistently, S and HE proteins are incorporated independent from each other. Direct interactions between S and HE were not observed when the proteins were coexpressed in cells (Nguyen and Hogue, 1997). This result is consistent with the idea that these proteins are separately drawn into the M protein lattice by their distinctive interactions with M molecules. It is also consistent with the concept that these proteins assume different positions within this lattice, a hypothesis based on the presumed different geometric requirements for the incorporation of trimeric and di- or tetrameric S and HE complexes, respectively.

How, in the face of this enormous flexibility in accommodating all these various numbers and combinations of viral components, do coronaviruses manage to maintain specificity? Host proteins have not been noticed to occur in virions, although this may simply not have been looked at carefully enough. By probing the specificity, using viral and nonviral membrane proteins, it appeared that foreign proteins are effectively excluded from coronaviral particles (de Haan *et al*., 2000). However, some missorting was found to occur, consistent with earlier observations (Yoshikura and Taguchi, 1978).

The picture of coronaviral envelope formation is one that is directed entirely by lateral interactions between the envelope proteins. In infected cells, membrane proteins—viral and cellular—are sampled for fit into the lattice formed by M molecules. The specificity of the molecular interactions acts as a quality control system to warrant the formation of the two-dimensional assemblies that contain the full complement of viral membrane proteins but from which cellular proteins are segregated. For each cellular protein the efficiency of this exclusion process is determined by its lack of interaction with the M protein, its lack of fit in the M protein framework, and its success in competing with the S and HE oligomers for the (geometrically different) vacancies within this framework.

3. Localization of Budding

The precise location of coronavirus budding and the factors that govern it have not been established. Although it is clear that particle formation occurs at membranes early in the secretory pathway, up to the *cis*-Golgi compartment, the precise site has not been identified for any coronavirus. Several considerations may explain this lack of

knowledge. One is that these early compartments are themselves rather complex and highly dynamic and have hence been difficult to define structurally. Another is the possible alteration of the structural integrity of these compartments by infection; studies of these effects have not been described. A third complication may be that coronaviruses do not behave uniformly, different viruses possibly preferring different membranes for budding. In this respect it may be of note that differences have been observed, for instance, in the intrinsic localization of the M proteins from IBV and MHV; they appeared to accumulate on the *cis* and *trans* side of the Golgi apparatus, respectively (Klumperman *et al*., 1994; Machamer *et al*., 1990).

It has long been assumed that the M protein determines the site of coronavirus budding. When, however, this protein appeared to localize beyond this site, the idea became attractive that the association of the envelope proteins may create the novel targeting signals that direct these multimeric complexes to the budding site. In support of such a notion is the fact that the S and HE proteins, when coexpressed with the M protein, are retained in the Golgi apparatus rather than being transported to the plasma membrane. The critical question now is whether and how the E protein affects the localization of the M protein. As the E protein by itself does not seem to localize to the virion budding site it will be of great interest to determine the membranes at which VLPs assemble.

As the envelope proteins can direct particle formation by themselves, it may seem that the nucleocapsid is not leading the assembly process. Still, besides giving rise to virions rather than VLPs, its involvement in assembly might have important consequences. First of all, nucleocapsids may enhance the efficiency of the budding process. The physical yields of VLPs obtained by coexpression of the envelope proteins in cells are generally poor. Although there may be many reasons for this, in infected cells the availability of nucleocapsids is likely to facilitate particle production. Empty particles, considered to be VLPs, have nevertheless been observed during natural infection (Afzelius, 1994; Macnaughton and Davies, 1980). Their formation might simply serve as a means to dispose of excess viral membrane proteins from infected cells if required.

Another effect of the nucleocapsid could involve the localization of budding. It is conceivable that, unless a defined budding station is created by a specific interplay between viral and host proteins (for which no indications yet exist), preassembled nucleocapsids dock at those intracellular membrane sites where sufficiently sized patches of M protein-based envelope structure have accumulated. Early in

infection such patches might start to form only after the envelope proteins have left the endoplasmic reticulum and become concentrated in intermediate membranes on their way to the Golgi complex. Later, when viral protein synthesis increases, this density might be reached earlier, perhaps explaining the observed late budding in the endoplasmic reticulum (Goldsmith *et al.*, 2004; Klumperman *et al.*, 1994; Tooze *et al.*, 1984). It will again be interesting to learn where VLPs independently bud and how this relates to the local density of the envelope proteins because this information will shed light on the role of the nucleocapsid in the localization of virion assembly.

V. PERSPECTIVES

The picture of coronavirus assembly that the available literature allows us to draw in this review is still a rough draft. We know the identity and some characteristics of the key elements of the picture, we know the relative positions and orientations of most of them, but we are unable to fit them all into a sensible composition.

Although this may seem like a discontented retrospective, it certainly is not. In the 25 years that the senior author has been in coronavirology research, enormous progress has been made in practically all its aspects including virion assembly. However, the rewarding act of compiling and ordering the available information and trying to abstract from it actual knowledge was at the same time a sharp and recurrent confrontation with the unknown. We want to conclude this work by summarizing what in our opinion will be the main issues for the near future.

With the obstacle of reverse genetics technology solved, "structure" will be the dominating issue of the next decade. Biology has taught that molecular insight into processes will eventually depend critically on detailed structural information. For coronavirus assembly this means data on the individual structural components and, particularly, on the virion. With respect to the former, this will be most challenging for the membrane proteins, notably M and E. Virions, by their apparent elasticity, have eluded structural analysis. Here, despite the still limited resolution to be expected, cryoelectron microscopy should provide the urgently required insight into the structural organization of the particle.

Another issue will be the cell biology of assembly. This actually refers to a number of poignant problems at every stage of the process. Starting with nucleocapsid formation we must admit that we know practically nothing. By which interactions and where on the genome

the packaging is initiated, how the wrapping of the RNA proceeds, how the condensation of the ribonucleoprotein structure takes place, and where in the cell these activities take place are all unresolved questions. Although we seem to know more about the budding process, several fundamental issues are still unresolved. Obvious issues are the site of budding and the determinants of its location, and the inclusion of the nucleocapsid into the budding particle. An intriguing issue is the budding mechanism itself: how is membrane curvature generated and, particularly, how is the directionality determined. Coronaviruses, like other intracellularly budding viruses, direct their particles out of the cytoplasm into the organelles, that is, opposite to the natural direction of cellular vesicle budding. Once again, simply nothing is known about the governing principles.

A third field of research that has yet to open is the contribution of host cellular factors to the assembly process. Work has so far been concentrating on the viral components and their interplay. Although there have been incidental indications, studies on the specific involvement of host proteins apparently had to await the development of appropriate technologies and these are now becoming available.

Although the serious health threat caused by the 2002–2003 epidemic of SARS apparently has waned, the coronavirological community has welcomed the consequent increased interest in this family of viruses. The boost that the research in this field has since been experiencing warrants an exciting future and accelerated progress with the elucidation of the fascinating process of coronavirus assembly.

Acknowledgments

We thank Henk Halsema for making most of the drawings. We are grateful to Cristina Risco for providing the electron micrographs demonstrating the structural maturation of virions; to Raoul de Groot, Berend Jan Bosch, and Jean Lepault for their combined efforts in providing the electron micrographs of the purified virions; and to Raoul de Groot for critical reading of the manuscript.

References

Afzelius, B. A. (1994). Ultrastructure of human nasal epithelium during an episode of coronavirus infection. *Virchows Arch.* **424:**295–300.

Allison, S. L., Stadler, K., Mandl, C. W., Kunz, C., and Heinz, F. X. (1995). Synthesis and secretion of recombinant tick-borne encephalitis virus protein E in soluble and particulate form. *J. Virol.* **69:**5816–5820.

An, S., Chen, C. J., Yu, X., Leibowitz, J. L., and Makino, S. (1999). Induction of apoptosis in murine coronavirus-infected cultured cells and demonstration of E protein as an apoptosis inducer. *J. Virol.* **73:**7853–7859.

Anderson, R., and Wong, F. (1993). Membrane and phospholipid binding by murine coronaviral nucleocapsid N protein. *Virology* **194:**224–232.

Armstrong, J., and Patel, S. (1991). The Golgi sorting domain of coronavirus E1 protein. *J. Cell Sci.* **98:**567–575.

Armstrong, J., Niemann, H., Smeekens, S., Rottier, P., and Warren, G. (1984). Sequence and topology of a model intracellular membrane protein, E1 glycoprotein, from a coronavirus. *Nature* **308:**751–752.

Armstrong, J., Patel, S., and Riddle, P. (1990). Lysosomal sorting mutants of coronavirus E1 protein, a Golgi membrane protein. *J. Cell Sci.* **95:**191–197.

Babcock, G. J., Esshaki, D. J., Thomas, W. D., and Ambrosino, D. M. (2004). Amino acids 270 to 510 of the severe acute respiratory syndrome coronavirus spike protein are required for interaction with receptor. *J. Virol.* **78:**4552–4560.

Baric, R. S., Nelson, G. W., Fleming, J. O., Deans, R. J., Keck, J. G., Casteel, N., and Stohlman, S. A. (1988). Interactions between coronavirus nucleocapsid protein and viral RNAs: Implications for viral transcription. *J. Virol.* **62:**4280–4287.

Baudoux, P., Besnardeau, L., Carrat, C., Rottier, P., Charley, B., and Laude, H. (1998a). Interferon α inducing property of coronavirus particles and pseudoparticles. *Adv. Exp. Med. Biol.* **440:**377–386.

Baudoux, P., Carrat, C., Besnardeau, L., Charley, B., and Laude, H. (1998b). Coronavirus pseudoparticles formed with recombinant M and E proteins induce α interferon synthesis by leukocytes. *J. Virol.* **72:**8636–8643.

Becker, W. B., McIntosh, K., Dees, J. H., and Chanock, R. M. (1967). Morphogenesis of avian infectious bronchitis virus and a related human virus (strain 229E). *J. Virol.* **1:**1019–1027.

Bisht, H., Roberts, A., Vogel, L., Bukreyev, A., Collins, P. L., Murphy, B. R., Subbarao, K., and Moss, B. (2004). Severe acute respiratory syndrome coronavirus spike protein expressed by attenuated vaccinia virus protectively immunizes mice. *Proc. Natl. Acad. Sci. USA* **101:**6641–6646.

Bonavia, A., Zelus, B. D., Wentworth, D. E., Talbot, P. J., and Holmes, K. V. (2003). Identification of a receptor-binding domain of the spike glycoprotein of human coronavirus HCoV-229E. *J. Virol.* **77:**2530–2538.

Bos, E. C., Dobbe, J. C., Luytjes, W., and Spaan, W. J. (1997). A subgenomic mRNA transcript of the coronavirus mouse hepatitis virus strain A59 defective interfering (DI) RNA is packaged when it contains the DI packaging signal. *J. Virol.* **71:**5684–5687.

Bos, E. C., Heijnen, L., Luytjes, W., and Spaan, W. J. (1995). Mutational analysis of the murine coronavirus spike protein: Effect on cell-to-cell fusion. *Virology* **214:**453–463.

Bos, E. C., Luytjes, W., van der Meulen, H. V., Koerten, H. K., and Spaan, W. J. (1996). The production of recombinant infectious DI-particles of a murine coronavirus in the absence of helper virus. *Virology* **218:**52–60.

Bosch, B. J., de Haan, C. A. M., and Rottier, P. J. M. (2004a). The coronavirus spike glycoprotein, extended carboxy terminally with the green fluorescent protein, is assembly competent. *J. Virol.* **78:**7369–7378.

Bosch, B. J., Martina, B. E., Van Der Zee, R., Lepault, J., Haijema, B. J., Versluis, C., Heck, A. J., De Groot, R., Osterhaus, A. D., and Rottier, P. J. (2004b). Severe acute respiratory syndrome coronavirus (SARS-CoV) infection inhibition using spike protein heptad repeat-derived peptides. *Proc. Natl. Acad. Sci. USA* **101:**8455–8460.

Bosch, B. J., van der Zee, R., de Haan, C. A., and Rottier, P. J. (2003). The coronavirus spike protein is a class I virus fusion protein: Structural and functional characterization of the fusion core complex. *J. Virol.* **77:**8801–8811.

Bost, A. G., Carnahan, R. H., Lu, X. T., and Denison, M. R. (2000). Four proteins processed from the replicase gene polyprotein of mouse hepatitis virus colocalize in the cell periphery and adjacent to sites of virion assembly. *J. Virol.* **74:**3379–3387.

Bost, A. G., Prentice, E., and Denison, M. R. (2001). Mouse hepatitis virus replicase protein complexes are translocated to sites of M protein accumulation in the ERGIC at late times of infection. *Virology* **285:**21–29.

Brayton, P. R., Ganges, R. G., and Stohlman, S. A. (1981). Host cell nuclear function and murine hepatitis virus replication. *J. Gen. Virol.* **56:**457–460.

Breslin, J. J., Mork, I., Smith, M. K., Vogel, L. K., Hemmila, E. M., Bonavia, A., Talbot, P. J., Sjostrom, H., Noren, O., and Holmes, K. V. (2003). Human coronavirus 229E: Receptor binding domain and neutralization by soluble receptor at 37 °C. *J. Virol.* **77:**4435–4438.

Brian, D. A., Hague, B. G., and Kienzle, T. E. (1995). The coronavirus hemagglutinin esterase glycoprotein. *In* "The *Coronaviridae*" (S. G. Siddell, ed.), pp. 165–179. Plenum Press, New York.

Bridger, J. C., Caul, E. O., and Egglestone, S. I. (1978). Replication of an enteric bovine coronavirus in intestinal organ cultures. *Arch. Virol.* **57:**43–51.

Brown, T. D. K., and Brierley, I. (1995). The coronavirus nonstructural proteins. *In* "The *Coronaviridae*" (S. G. Siddell, ed.), pp. 191–217. Plenum Press, New York.

Caul, E. O., Ashley, C. R., Ferguson, N. M., and Egglestone, S. I. (1979). Preliminary studies on the isolation of coronavirus 229E nucleocapsids. *FEMS Microbiol. Lett.* **48:**193.

Caul, E. O., and Egglestone, S. I. (1977). Further studies on human enteric coronaviruses. *Arch. Virol.* **54:**107–117.

Cavanagh, D. (1983a). Coronavirus IBV: Further evidence that the surface projections are associated with two glycopolypeptides. *J. Gen. Virol.* **64:**1787–1791.

Cavanagh, D. (1983b). Coronavirus IBV: Structural characterization of the spike protein. *J. Gen. Virol.* **64:**2577–2583.

Cavanagh, D. (1995). The coronavirus surface glycoprotein. *In* "The *Coronaviridae*" (S. G. Siddell, ed.), pp. 73–113. Plenum Press, New York.

Cavanagh, D., Davis, P. J., and Pappin, D. J. (1986). Coronavirus IBV glycopolypeptides: Locational studies using proteases and saponin, a membrane permeablizer. *Virus Res.* **4:**145–156.

Chambers, P., Pringle, C. R., and Easton, A. J. (1990). Heptad repeat sequences are located adjacent to hydrophobic regions in several types of virus fusion glycoproteins. *J. Gen. Virol.* **71:**3075–3080.

Chang, K. W., and Gombold, J. L. (2001). Effects of amino acid insertions in the cysteine-rich domain of the MHV-A59 spike protein on cell fusion. *Adv. Exp. Med. Biol.* **494:**205–211.

Chang, K. W., Sheng, Y., and Gombold, J. L. (2000). Coronavirus-induced membrane fusion requires the cysteine-rich domain in the spike protein. *Virology* **269:**212–224.

Chang, R. Y., and Brian, D. A. (1996). *Cis* requirement for N-specific protein sequence in bovine coronavirus defective interfering RNA replication. *J. Virol.* **70:**2201–2207.

Charley, B., and Laude, H. (1988). Induction of α interferon by transmissible gastroenteritis coronavirus: Role of transmembrane glycoprotein E1. *J. Virol.* **62:**8–11.

Chasey, D., and Alexander, D. J. (1976). Morphogenesis of avian infectious bronchitis virus in primary chick kidney cells. *Arch. Virol.* **52:**101–111.

Chen, H., Wurm, T., Britton, P., Brooks, G., and Hiscox, J. A. (2002). Interaction of the coronavirus nucleoprotein with nucleolar antigens and the host cell. *J. Virol.* **76:**5233–5250.

Choi, K. S., Huang, P., and Lai, M. M. (2002). Polypyrimidine-tract-binding protein affects transcription but not translation of mouse hepatitis virus RNA. *Virology* **303:**58–68.

Cologna, R., and Hogue, B. G. (2000). Identification of a bovine coronavirus packaging signal. *J. Virol.* **74:**580–583.

Cologna, R., Spagnolo, J. F., and Hogue, B. G. (2000). Identification of nucleocapsid binding sites within coronavirus-defective genomes. *Virology* **277:**235–249.

Compton, S. R., Rogers, D. B., Holmes, K. V., Fertsch, D., Remenick, J., and McGowan, J. J. (1987). *In vitro* replication of mouse hepatitis virus strain A59. *J. Virol.* **61:**1814–1820.

Cornelissen, L. A. H. M., Wierda, C. M. H., van der Meer, F. J., Herrewegh, A. A. P. M., Horzinek, M. C., Egberink, H. F., and de Groot, R. J. (1997). Hemagglutinin-esterase, a novel structural protein of torovirus. *J. Virol.* **71:**5277–5286.

Corse, E., and Machamer, C. E. (2000). Infectious bronchitis virus E protein is targeted to the Golgi complex and directs release of virus-like particles. *J. Virol.* **74:**4319–4326.

Corse, E., and Machamer, C. E. (2002). The cytoplasmic tail of infectious bronchitis virus E protein directs Golgi targeting. *J. Virol.* **76:**1273–1284.

Corse, E., and Machamer, C. E. (2003). The cytoplasmic tails of infectious bronchitis virus E and M proteins mediate their interaction. *Virology* **312:**25–34.

Curtis, K. M., Yount, B., and Baric, R. S. (2002). Heterologous gene expression from transmissible gastroenteritis virus replicon particles. *J. Virol.* **76:**1422–1434.

Dalton, K., Casais, R., Shaw, K., Stirrups, K., Evans, S., Britton, P., Brown, T. D., and Cavanagh, D. (2001). *Cis*-acting sequences required for coronavirus infectious bronchitis virus defective-RNA replication and packaging. *J. Virol.* **75:**125–133.

David-Ferreira, J. F., and Manaker, R. A. (1965). An electron microscopic study of the development of a mouse hepatitis virus in tissue culture cells. *J. Cell Biol.* **24:**57–78.

Davies, H. A., Dourmashkin, R. R., and Macnaughton, M. R. (1981). Ribonucleoprotein of avian infectious bronchitis virus. *J. Gen. Virol.* **53:**67–74.

de Groot, R. J., Lenstra, J. A., Luytjes, W., Niesters, H. G., Horzinek, M. C., van der Zeijst, B. A., and Spaan, W. J. (1987a). Sequence and structure of the coronavirus peplomer protein. *Adv. Exp. Med. Biol.* **218:**31–38.

de Groot, R. J., Luytjes, W., Horzinek, M. C., van der Zeist, B. A., Spaan, W. J., and Lenstra, J. A. (1987b). Evidence for a coiled-coil structure in the spike proteins of coronaviruses. *J. Mol. Biol.* **196:**963–966.

de Groot, R. J., van Leen, R. W., Dalderup, M. J., Vennema, H., Horzinek, M. C., and Spaan, W. J. (1989). Stably expressed FIPV peplomer protein induces cell fusion and elicits antibodies in mice. *Virology* **171:**493.

de Haan, C. A., de Wit, M., Kuo, L., Montalto-Morrison, C., Haagmans, B. L., Weiss, S. R., Masters, P. S., and Rottier, P. J. (2003). The glycosylation status of the murine hepatitis coronavirus M protein affects the interferogenic capacity of the virus *in vitro* and its ability to replicate in the liver but not the brain. *Virology* **312:**395–406.

de Haan, C. A., Kuo, L., Masters, P. S., Vennema, H., and Rottier, P. J. (1998a). Coronavirus particle assembly: Primary structure requirements of the membrane protein. *J. Virol.* **72:**6838–6850.

de Haan, C. A., Masters, P. S., Shen, X., Weiss, S., and Rottier, P. J. (2002b). The group-specific murine coronavirus genes are not essential, but their deletion, by reverse genetics, is attenuating in the natural host. *Virology* **296:**177–189.

de Haan, C. A., Roestenberg, P., de Wit, M., de Vries, A. A., Nilsson, T., Vennema, H., and Rottier, P. J. (1998b). Structural requirements for O-glycosylation of the mouse hepatitis virus membrane protein. *J. Biol. Chem.* **273:**29905–29914.

de Haan, C. A., Smeets, M., Vernooij, F., Vennema, H., and Rottier, P. J. (1999). Mapping of the coronavirus membrane protein domains involved in interaction with the spike protein. *J. Virol.* **73:**7441–7452.

de Haan, C. A., Vennema, H., and Rottier, P. J. (2000). Assembly of the coronavirus envelope: Homotypic interactions between the M proteins. *J. Virol.* **74:**4967–4978.

de Haan, C. A., de Wit, M., Kuo, L., Montalto, C., Masters, P. S., Weiss, S. R., and Rottier, P. J. (2002a). O-glycosylation of the mouse hepatitis coronavirus membrane protein. *Virus Res.* **82:**77–81.

de Haan, C. A. M., Stadler, K., Godeke, G.-J., Bosch, B. J., and Rottier, P. J. M. (2004). Cleavage inhibition of the murine coronavirus spike protein by a furin-like enzyme affects cell–cell but not virus–cell fusion. *J. Virol.* **78:**6048–6054.

de Vries, A. A., Horzinek, M. C., Rottier, P. J., and de Groot, R. J. (1997). The genome organization of the nidovirales: Similarities and differences between arteri-, toro-, and coronaviruses. *Semin. Virol.* **8:**33–47.

Delmas, B., Gelfi, J., L'Haridon, R., Vogel, L. K., Sjostrom, H., Noren, O., and Laude, H. (1992). Aminopeptidase N is a major receptor for the entero-pathogenic coronavirus TGEV. *Nature* **357:**417–420.

Delmas, B., Gelfi, J., Sjostrom, H., Noren, O., and Laude, H. (1993). Further characterization of aminopeptidase-N as a receptor for coronaviruses. *Adv. Exp. Med. Biol.* **342:**293–298.

Delmas, B., and Laude, H. (1990). Assembly of coronavirus spike protein into trimers and its role in epitope expression. *J. Virol.* **64:**5367–5375.

Denison, M. R., Spaan, W. J., van der Meer, Y., Gibson, C. A., Sims, A. C., Prentice, E., and Lu, X. T. (1999). The putative helicase of the coronavirus mouse hepatitis virus is processed from the replicase gene polyprotein and localizes in complexes that are active in viral RNA synthesis. *J. Virol.* **73:**6862–6871.

Deregt, D., and Babiuk, L. A. (1987). Monoclonal antibodies to bovine coronavirus: Characteristics and topographical mapping of neutralizing epitopes on the E2 and E3 glycoproteins. *Virology* **161:**410–420.

Doms, R., Lamb, R. A., Rose, J. K., and Helenius, A. (1993). Folding and assembly of viral membrane proteins. *Virology* **193:**545–562.

Dubois-Dalcq, M. E., Doller, E. W., Haspel, M. V., and Holmes, K. V. (1982). Cell tropism and expression of mouse hepatitis viruses (MHV) in mouse spinal cord cultures. *Virology* **119:**317–331.

Dveksler, G. S., Dieffenbach, C. W., Cardellichio, C. B., McCuaig, K., Pensiero, M. N., Jiang, G. S., Beauchemin, N., and Holmes, K. V. (1993). Several members of the mouse carcinoembryonic antigen-related glycoprotein family are functional receptors for the coronavirus mouse hepatitis virus-A59. *J. Virol.* **67:**1–8.

Dveksler, G. S., Pensiero, M. N., Cardellichio, C. B., Williams, R. K., Jiang, G. S., Holmes, K. V., and Dieffenbach, C. W. (1991). Cloning of the mouse hepatitis virus (MHV) receptor: Expression in human and hamster cell lines confers susceptibility to MHV. *J. Virol.* **65:**6881–6891.

Eleouet, J. F., Slee, E. A., Saurini, F., Castagne, N., Poncet, D., Garrido, C., Solary, E., and Martin, S. J. (2000). The viral nucleocapsid protein of transmissible gastroenteritis coronavirus (TGEV) is cleaved by caspase-6 and -7 during TGEV-induced apoptosis. *J. Virol.* **74:**3975–3983.

Enjuanes, L., Sola, I., Almazan, F., Ortego, J., Izeta, A., Gonzalez, J. M., Alonso, S., Sanchez, J. M., Escors, D., Calvo, E., Riquelme, C., and Sanchez, C. (2001). Coronavirus derived expression systems. *J. Biotechnol.* **88:**183–204.

Escors, D., Camafeita, E., Ortego, J., Laude, H., and Enjuanes, L. (2001a). Organization of two transmissible gastroenteritis coronavirus membrane protein topologies within the virion and core. *J. Virol.* **75:**12228–12240.

Escors, D., Izeta, A., Capiscol, C., and Enjuanes, L. (2003). Transmissible gastroenteritis coronavirus packaging signal is located at the 5′ end of the virus genome. *J. Virol.* **77:**7890–7902.

Escors, D., Ortego, J., Laude, H., and Enjuanes, L. (2001b). The membrane M protein carboxy terminus binds to transmissible gastroenteritis coronavirus core and contributes to core stability. *J. Virol.* **75:**1312–1324.

Fischer, F., Peng, D., Hingley, S. T., Weiss, S. R., and Masters, P. S. (1997). The internal open reading frame within the nucleocapsid gene of mouse hepatitis virus encodes a structural protein that is not essential for viral replication. *J. Virol.* **71:**996–1003.

Fischer, F., Stegen, C. F., Masters, P. S., and Samsonoff, W. A. (1998). Analysis of constructed E gene mutants of mouse hepatitis virus confirms a pivotal role for E protein in coronavirus assembly. *J. Virol.* **72:**7885–7894.

Fosmire, J. A., Hwang, K., and Makino, S. (1992). Identification and characterization of a coronavirus packaging signal. *J. Virol.* **66:**3522–3530.

Frana, M. F., Behnke, J. N., Sturman, L. S., and Holmes, K. V. (1985). Proteolytic cleavage of the E2 glycoprotein of murine coronavirus: Host-dependent differences in proteolytic cleavage and cell fusion. *J. Virol.* **56:**912–920.

Gagneten, S., Gout, O., Dubois-Dalcq, M., Rottier, P., Rossen, J., and Holmes, K. V. (1995). Interaction of mouse hepatitis virus (MHV) spike glycoprotein with receptor glycoprotein MHVR is required for infection with an MHV strain that expresses the hemagglutinin-esterase glycoprotein. *J. Virol.* **69:**889–895.

Gallagher, T. M. (1997). A role for naturally occurring variation of the murine coronavirus spike protein in stabilizing association with the cellular receptor. *J. Virol.* **71:**3129–3137.

Gallagher, T. M., and Buchmeier, M. J. (2001). Coronavirus spike proteins in viral entry and pathogenesis. *Virology* **279:**371–374.

Gallagher, T. M., Buchmeier, M. J., and Perlman, S. (1992). Cell receptor-independent infection by a neurotropic murine coronavirus. *Virology* **191:**517–522.

Gallagher, T. M., Escarmis, C., and Buchmeier, M. J. (1991). Alteration of the pH dependence of coronavirus-induced cell fusion: Effect of mutations in the spike glycoprotein. *J. Virol.* **65:**1916–1928.

Garoff, H., Hewson, R., and Opstelten, D. J. (1998). Virus maturation by budding. *Microbiol. Mol. Biol. Rev.* **62:**1171–1190.

Garwes, D. J., Bountiff, L., Millson, G. C., and Elleman, C. J. (1984). Defective replication of porcine transmissible gastroenteritis virus in a continuous cell line. *Adv. Exp. Med. Biol.* **173:**79–93.

Garwes, D. J., Pocock, D. H., and Pike, B. V. (1976). Isolation of subviral components from transmissible gastroenteritis virus. *J. Gen. Virol.* **32:**283–294.

Godeke, G. J., de Haan, C. A., Rossen, J. W., Vennema, H., and Rottier, P. J. (2000). Assembly of spikes into coronavirus particles is mediated by the carboxy-terminal domain of the spike protein. *J. Virol.* **74:**1566–1571.

Godet, M., Grosclaude, J., Delmas, B., and Laude, H. (1994). Major receptor-binding and neutralization determinants are located within the same domain of the transmissible gastroenteritis virus (coronavirus) spike protein. *J. Virol.* **68:**8008–8016.

Godet, M., L'Haridon, R., Vautherot, J. F., and Laude, H. (1992). TGEV corona virus ORF4 encodes a membrane protein that is incorporated into virions. *Virology* **188:**666–675.

Goldsmith, C., Tatti, K., Ksiazek, T., Rollin, P., Comer, J., Lee, W., Rota, P., Bankamp, B., Bellini, W., and Zaki, S. (2004). Ultrastructural characterization of SARS coronavirus. *Emerg. Infect. Dis.* **10:**320–326.

Gonzalez, M. E., and Carrasco, L. (2003). Viroporins. *FEBS Lett.* **552:**28–34.

Gosert, R., Kanjanahaluethai, A., Egger, D., Bienz, K., and Baker, S. C. (2002). RNA replication of mouse hepatitis virus takes place at double-membrane vesicles. *J. Virol.* **76:**3697–3708.

Haijema, B. J., Volders, H., and Rottier, P. J. (2003). Switching species tropism: An effective way to manipulate the feline coronavirus genome. *J. Virol.* **77:**4528–4538.

Haijema, B. J., Volders, H., and Rottier, P. J. (2004). Live, attenuated coronavirus vaccines through the directed deletion of group-specific genes provide protection against feline infectious peritonitis. *J. Virol.* **78:**3863–3871.

Hamre, D., Kindig, D. A., and Mann, J. (1967). Growth and intracellular development of a new respiratory virus. *J. Virol.* **1:**810–816.

He, R., Dobie, F., Ballantine, M., Leeson, A., Li, Y., Bastien, N., Cutts, T., Andonov, A., Cao, J., Booth, T. F., Plummer, F. A., Tyler, S., Baker, L., and Li, X. (2004). Analysis of multimerization of the SARS coronavirus nucleocapsid protein. *Biochem. Biophys. Res. Commun.* **316:**476–483.

Herrewegh, A. A., Vennema, H., Horzinek, M. C., Rottier, P. J., and de Groot, R. J. (1995). The molecular genetics of feline coronaviruses: Comparative sequence analysis of the ORF7a/7b transcription unit of different biotypes. *Virology* **212:**622–631.

Hiscox, J. A., Wurm, T., Wilson, L., Britton, P., Cavanagh, D., and Brooks, G. (2001). The coronavirus infectious bronchitis virus nucleoprotein localizes to the nucleolus. *J. Virol.* **75:**506–512.

Hofmann, M. A., Sethna, P. B., and Brian, D. A. (1990). Bovine coronavirus mRNA replication continues throughout persistent infection in cell culture. *J. Virol.* **64:**4108–4114.

Hogue, B. G., and Brian, D. A. (1986). Structural proteins of human respiratory coronavirus OC43. *Virus Res.* **5:**131–144.

Hogue, B. G., Kienzle, T. E., and Brian, D. A. (1989). Synthesis and processing of the bovine enteric coronavirus haemagglutinin protein. *J. Gen. Virol.* **70:**345–352.

Hogue, B. G., King, B., and Brian, D. A. (1984). Antigenic relationships among proteins of bovine coronavirus, human respiratory coronavirus OC43, and mouse hepatitis coronavirus A59. *J. Virol.* **51:**384–388.

Holmes, K. V. (2001). Enteric infections with coronaviruses and toroviruses. *Novartis Found. Symp.* **238:**258–269; discussion 269–275.

Holmes, K. V., and Behnke, J. N. (1981). Evolution of a coronavirus during persistent infection *in vitro*. *Adv. Exp. Med. Biol.* **142:**287–299.

Holmes, K. V., Doller, E. W., and Sturman, L. S. (1981). Tunicamycin resistant glycosylation of coronavirus glycoprotein: Demonstration of a novel type of viral glycoprotein. *Virology* **115:**334–344.

Holmes, K. V., Zelus, B. D., Schickli, J. H., and Weiss, S. R. (2001). Receptor specificity and receptor-induced conformational changes in mouse hepatitis virus spike glycoprotein. *Adv. Exp. Med. Biol.* **494:**173–181.

Huang, Q., Yu, L., Petros, A. M., Gunasekera, A., Liu, Z., Xu, N., Hajduk, P., Mack, J., Fesik, S. W., and Olejniczak, E. T. (2004). Structure of the N-terminal RNA-binding domain of the SARS CoV nucleocapsid protein. *Biochemistry* **43:**6059–6063.

Ingallinella, P., Bianchi, E., Finotto, M., Cantoni, G., Eckert, D. M., Supekar, V. M., Bruckmann, C., Carfi, A., and Pessi, A. (2004). Structural characterization of the fusion-active complex of severe acute respiratory syndrome (SARS) coronavirus. *Proc. Natl. Acad. Sci. USA* **101:**8709–8714.

Izeta, A., Smerdou, C., Alonso, S., Penzes, Z., Mendez, A., Plana-Duran, J., and Enjuanes, L. (1999). Replication and packaging of transmissible gastroenteritis coronavirus-derived synthetic minigenomes. *J. Virol.* **73:**1535–1545.

Kalicharran, K., Mohandas, D., Wilson, G., and Dales, S. (1996). Regulation of the initiation of coronavirus JHM infection in primary oligodendrocytes and L-2 fibroblasts. *Virology* **225:**33–43.

Kennedy, D. A., and Johnson-Lussenburg, C. M. (1975). Isolation and morphology of the internal component of human coronavirus, strain 229E. *InterVirology* **6:**197–206.

Kennedy, M., Boedeker, N., Gibbs, P., and Kania, S. (2001). Deletions in the 7a ORF of feline coronavirus associated with an epidemic of feline infectious peritonitis. *Vet. Microbiol.* **81:**227–234.

Kienzle, T. E., Abraham, S., Hogue, B. G., and Brian, D. A. (1990). Structure and orientation of expressed bovine coronavirus hemagglutinin-esterase protein. *J. Virol.* **64:**1834–1838.

Kim, K. H., Narayanan, K., and Makino, S. (1997). Assembled coronavirus from complementation of two defective interfering RNAs. *J. Virol.* **71:**3922–3931.

King, B., Potts, B. J., and Brian, D. A. (1985). Bovine coronavirus hemagglutinin protein. *Virus Res.* **2:**53–59.

Klausegger, A., Strobl, B., Regl, G., Kaser, A., Luytjes, W., and Vlasak, R. (1999). Identification of a coronavirus hemagglutinin-esterase with a substrate specificity different from those of influenza C virus and bovine coronavirus. *J. Virol.* **73:**3737–3743.

Klumperman, J., Locker, J. K., Meijer, A., Horzinek, M. C., Geuze, H. J., and Rottier, P. J. (1994). Coronavirus M proteins accumulate in the Golgi complex beyond the site of virion budding. *J. Virol.* **68:**6523–6534.

Koetzner, C. A., Parker, M. M., Ricard, C. S., Sturman, L. S., and Masters, P. S. (1992). Repair and mutagenesis of the genome of a deletion mutant of the coronavirus mouse hepatitis virus by targeted RNA recombination. *J. Virol.* **66:**1841–1848.

Krempl, C., Schultze, B., and Herrler, G. (1995). Analysis of cellular receptors for human coronavirus OC43. *Adv. Exp. Med. Biol.* **380:**371–374.

Krueger, D. K., Kelly, S. M., Lewicki, D. N., Ruffolo, R., and Gallagher, T. M. (2001). Variations in disparate regions of the murine coronavirus spike protein impact the initiation of membrane fusion. *J. Virol.* **75:**2792–2802.

Kubo, H., Yamada, Y. K., and Taguchi, F. (1994). Localization of neutralizing epitopes and the receptor-binding site within the amino-terminal 330 amino acids of the murine coronavirus spike protein. *J. Virol.* **68:**5403–5410.

Kunkel, F., and Herrler, G. (1993). Structural and functional analysis of the surface protein of human coronavirus OC43. *Virology* **195:**195–202.

Kuo, L., and Masters, P. S. (2002). Genetic evidence for a structural interaction between the carboxy termini of the membrane and nucleocapsid proteins of mouse hepatitis virus. *J. Virol.* **76:**4987–4999.

Kuo, L., Godeke, G. J., Raamsman, M. J., Masters, P. S., and Rottier, P. J. (2000). Retargeting of coronavirus by substitution of the spike glycoprotein ectodomain: Crossing the host cell species barrier. *J. Virol.* **74:**1393–1406.

Kuo, L., and Masters, P. S. (2003). The small envelope protein E is not essential for murine coronavirus replication. *J. Virol.* **77:**4597–4608.

Lai, M. M. (1997). RNA–protein interactions in the regulation of coronavirus RNA replication and transcription. *Biol. Chem.* **378:**477–481.

Lai, M. M., and Cavanagh, D. (1997). The molecular biology of coronaviruses. *Adv. Virus Res.* **48:**1–100.

Lai, M. M., Liao, C. L., Lin, Y. J., and Zhang, X. (1994). Coronavirus: How a large RNA viral genome is replicated and transcribed. *Infect. Agents Dis.* **3:**98–105.

Lancer, J. A., and Howard, C. R. (1980). The disruption of infectious bronchitis virus (IBV-41 strain) with Triton X-100 detergent. *J. Virol. Methods* **1:**121–131.

Laude, H., Gelfi, J., Lavenant, L., and Charley, B. (1992). Single amino acid changes in the viral glycoprotein M affect induction of α interferon by the coronavirus transmissible gastroenteritis virus. *J. Virol.* **66:**743–749.

Laude, H., and Masters, P. S. (1995). The coronavirus nucleocapsid protein. *In* "The *Coronaviridae*" (S. G. Siddell, ed.), pp. 141–163. Plenum Press, New York.

Lewicki, D. N., and Gallagher, T. M. (2002). Quaternary structure of coronavirus spikes in complex with carcinoembryonic antigen-related cell adhesion molecule cellular receptors. *J. Biol. Chem.* **277:**19727–19734.

Li, W., Moore, M. J., Vasilieva, N., Sui, J., Wong, S. K., Berne, M. A., Somasundaran, M., Sullivan, J. L., Luzuriaga, K., Greenough, T. C., Choe, H., and Farzan, M. (2003). Angiotensin-converting enzyme 2 is a functional receptor for the SARS coronavirus. *Nature* **426:**450–454.

Liao, C. L., Zhang, X., and Lai, M. M. (1995). Coronavirus defective-interfering RNA as an expression vector: The generation of a pseudorecombinant mouse hepatitis virus expressing hemagglutinin-esterase. *Virology* **208:**319–327.

Lim, K. P., and Liu, D. X. (2001). The missing link in coronavirus assembly. Retention of the avian coronavirus infectious bronchitis virus envelope protein in the pre-Golgi compartments and physical interaction between the envelope and membrane proteins. *J. Biol. Chem.* **276:**17515–17523.

Lin, Y., Yan, X., Cao, W., Wang, C., Feng, J., Duan, J., and Xie, S. (2004). Probing the structure of the SARS coronavirus using scanning electron microscopy. *Antiviral Ther.* **9:**287–289.

Liu, D. X., and Inglis, S. C. (1991). Association of the infectious bronchitis virus 3c protein with the virion envelope. *Virology* **185:**911–917.

Liu, S., Xiao, G., Chen, Y., He, Y., Niu, J., Escalante, C. R., Xiong, H., Farmar, J., Debnath, A. K., Tien, P., and Jiang, S. (2004). Interaction between heptad repeat 1 and 2 regions in spike protein of SARS-associated coronavirus: Implications for virus fusogenic mechanism and identification of fusion inhibitors. *Lancet* **363:**938–947.

Locker, J. K., Griffiths, G., Horzinek, M. C., and Rottier, P. J. (1992). O-glycosylation of the coronavirus M protein. Differential localization of sialyltransferases in N- and O-linked glycosylation. *J. Biol. Chem.* **267:**14094–14101.

Locker, J. K., Klumperman, J., Oorschot, V., Horzinek, M. C., Geuze, H. J., and Rottier, P. J. (1994). The cytoplasmic tail of mouse hepatitis virus M protein is essential but not sufficient for its retention in the Golgi complex. *J. Biol. Chem.* **269:**28263–28269.

Locker, J. K., Opstelten, D. J., Ericsson, M., Horzinek, M. C., and Rottier, P. J. (1995). Oligomerization of a *trans*-Golgi/*trans*-Golgi network retained protein occurs in the Golgi complex and may be part of its retention. *J. Biol. Chem.* **270:**8815–8821.

Lontok, E., Corse, E., and Machamer, C. E. (2004). Intracellular targeting signals contribute to localization of coronavirus spike proteins near the virus assembly site. *J. Virol.* **78:**5913–5922.

Luo, Z., Matthews, A. M., and Weiss, S. R. (1999). Amino acid substitutions within the leucine zipper domain of the murine coronavirus spike protein cause defects in oligomerization and the ability to induce cell-to-cell fusion. *J. Virol.* **73:**8152–8159.

Luo, Z., and Weiss, S. R. (1998). Roles in cell-to-cell fusion of two conserved hydrophobic regions in the murine coronavirus spike protein. *Virology* **244:**483–494.

Luytjes, W. (1995). Coronavirus gene expression. *In* "The *Coronaviridae*" (S. G. Siddell, ed.), pp. 33–54. Plenum Press, New York.

Luytjes, W., Bredenbeek, P. J., Noten, A. F., Horzinek, M. C., and Spaan, W. J. (1988). Sequence of mouse hepatitis virus A59 mRNA 2: Indications for RNA recombination between coronaviruses and influenza C virus. *Virology* **166:**415–422.

Luytjes, W., Gerritsma, H., Bos, E., and Spaan, W. (1997). Characterization of two temperature-sensitive mutants of coronavirus mouse hepatitis virus strain A59 with maturation defects in the spike protein. *J. Virol.* **71:**949–955.

Maceyka, M., and Machamer, C. E. (1997). Ceramide accumulation uncovers a cycling pathway for the *cis*-Golgi network marker, infectious bronchitis virus M protein. *J. Cell Biol.* **139:**1411–1418.

Machamer, C. E., Grim, M. G., Esquela, A., Chung, S. W., Rolls, M., Ryan, K., and Swift, A. M. (1993). Retention of a *cis* Golgi protein requires polar residues on one face of a predicted α-helix in the transmembrane domain. *Mol. Biol. Cell* **4:**695–704.

Machamer, C. E., Mentone, S. A., Rose, J. K., and Farquhar, M. G. (1990). The E1 glycoprotein of an avian coronavirus is targeted to the *cis* Golgi complex. *Proc. Natl. Acad. Sci. USA* **87:**6944–6948.

Machamer, C. E., and Rose, J. K. (1987). A specific transmembrane domain of a coronavirus E1 glycoprotein is required for its retention in the Golgi region. *J. Cell Biol.* **105:**1205–1214.

Macnaughton, M. R., and Davies, H. A. (1978). Ribonucleoprotein-like structures from coronavirus particles. *J. Gen. Virol.* **39:**545–549.

Macnaughton, M. R., and Davies, H. A. (1980). Two particle types of avian infectious bronchitis virus. *J. Gen. Virol.* **47:**365–372.

Maeda, J., Maeda, A., and Makino, S. (1999). Release of coronavirus E protein in membrane vesicles from virus-infected cells and E protein-expressing cells. *Virology* **263:**265–272.

Maeda, J., Repass, J. F., Maeda, A., and Makino, S. (2001). Membrane topology of coronavirus E protein. *Virology* **281:**163–169.

Mason, P. W., Pincus, S., Fournier, M. J., Mason, T. L., Shope, R. E., and Paoletti, E. (1991). Japanese encephalitis virus–vaccinia recombinants produce particulate forms of the structural membrane proteins and induce high levels of protection against lethal JEV infection. *Virology* **180:**294–305.

Massalski, A., Coulter-Mackie, M., Knobler, R. L., Buchmeier, M. J., and Dales, S. (1982). *In vivo* and *in vitro* models of demyelinating diseases. V. Comparison of the assembly of mouse hepatitis virus, strain JHM, in two murine cell lines. *InterVirology* **18:**135–146.

Masters, P. S. (1992). Localization of an RNA-binding domain in the nucleocapsid protein of the coronavirus mouse hepatitis virus. *Arch. Virol.* **125:**141–160.

Masters, P. S. (1999). Reverse genetics of the largest RNA viruses. *Adv. Virus Res.* **53:**245–264.

Matsuyama, S., and Taguchi, F. (2002). Receptor-induced conformational changes of murine coronavirus spike protein. *J. Virol.* **76:**11819–11826.

Mayer, T., Tamura, T., Falk, M., and Niemann, H. (1988). Membrane integration and intracellular transport of the coronavirus glycoprotein E1, a class III membrane glycoprotein. *J. Biol. Chem.* **263:**14956–14963.

Miura, H. S., Nakagaki, K., and Taguchi, F. (2004). N-terminal domain of the murine coronavirus receptor CEACAM1 is responsible for fusogenic activation and conformational changes of the spike protein. *J. Virol.* **78:**216–223.

Mohandas, D. V., and Dales, S. (1991). Endosomal association of a protein phosphatase with high dephosphorylating activity against a coronavirus nucleocapsid protein. *FEBS Lett.* **282:**419–424.

Molenkamp, R., and Spaan, W. J. (1997). Identification of a specific interaction between the coronavirus mouse hepatitis virus A59 nucleocapsid protein and packaging signal. *Virology* **239:**78–86.

Mounir, S., and Talbot, P. J. (1992). Sequence analysis of the membrane protein gene of human coronavirus OC43 and evidence for O-glycosylation. *J. Gen. Virol.* **73:**2731–2736.

Narayanan, K., Chen, C. J., Maeda, J., and Makino, S. (2003a). Nucleocapsid-independent specific viral RNA packaging via viral envelope protein and viral RNA signal. *J. Virol.* **77:**2922–2927.

Narayanan, K., Kim, K. H., and Makino, S. (2003b). Characterization of N protein self-association in coronavirus ribonucleoprotein complexes. *Virus Res.* **98:**131–140.

Narayanan, K., Maeda, A., Maeda, J., and Makino, S. (2000). Characterization of the coronavirus M protein and nucleocapsid interaction in infected cells. *J. Virol.* **74:**8127–8134.

Narayanan, K., and Makino, S. (2001). Cooperation of an RNA packaging signal and a viral envelope protein in coronavirus RNA packaging. *J. Virol.* **75:**9059–9067.

Nelson, G. W., and Stohlman, S. A. (1993). Localization of the RNA-binding domain of mouse hepatitis virus nucleocapsid protein. *J. Gen. Virol.* **74:**1975–1979.

Nelson, G. W., Stohlman, S. A., and Tahara, S. M. (2000). High affinity interaction between nucleocapsid protein and leader/intergenic sequence of mouse hepatitis virus RNA. *J. Gen. Virol.* **81:**181–188.

Nguyen, V. P., and Hogue, B. G. (1997). Protein interactions during coronavirus assembly. *J. Virol.* **71:**9278–9284.

Opstelten, D. J., de Groote, P., Horzinek, M. C., Vennema, H., and Rottier, P. J. (1993a). Disulfide bonds in folding and transport of mouse hepatitis coronavirus glycoproteins. *J. Virol.* **67:**7394–7401.

Opstelten, D. J., Horzinek, M. C., and Rottier, P. J. (1993b). Complex formation between the spike protein and the membrane protein during mouse hepatitis virus assembly. *Adv. Exp. Med. Biol.* **342:**189–195.

Opstelten, D. J., Raamsman, M. J., Wolfs, K., Horzinek, M. C., and Rottier, P. J. (1995). Envelope glycoprotein interactions in coronavirus assembly. *J. Cell Biol.* **131:**339–349.

Ortego, J., Escors, D., Laude, H., and Enjuanes, L. (2002). Generation of a replication-competent, propagation-deficient virus vector based on the transmissible gastroenteritis coronavirus genome. *J. Virol.* **76:**11518–11529.

Ortego, J., Sola, I., Almazan, F., Ceriani, J. E., Riquelme, C., Balasch, M., Plana, J., and Enjuanes, L. (2003). Transmissible gastroenteritis coronavirus gene 7 is not essential but influences *in vivo* virus replication and virulence. *Virology* **308:**13–22.

Oshiro, L. S., Schieble, J. H., and Lennette, E. H. (1971). Electron microscopic studies of coronavirus. *J. Gen. Virol.* **12:**161–168.

Parker, M. D., Cox, G. J., Deregt, D., Fitzpatrick, D. R., and Babiuk, L. A. (1989). Cloning and *in vitro* expression of the gene for the E3 haemagglutinin glycoprotein of bovine coronavirus. *J. Gen. Virol.* **70:**155–164.

Parker, M. M., and Masters, P. S. (1990). Sequence comparison of the N genes of five strains of the coronavirus mouse hepatitis virus suggests a three domain structure for the nucleocapsid protein. *Virology* **179:**463–468.

Patzer, E. J., Nakamura, G. R., Simonsen, C. C., Levinson, A. D., and Brands, R. (1986). Intracellular assembly and packaging of hepatitis B surface antigen particles occur in the endoplasmic reticulum. *J. Virol.* **58:**884–892.

Peng, D., Koetzner, C. A., and Masters, P. S. (1995a). Analysis of second-site revertants of a murine coronavirus nucleocapsid protein deletion mutant and construction of nucleocapsid protein mutants by targeted RNA recombination. *J. Virol.* **69:**3449–3457.

Peng, D., Koetzner, C. A., McMahon, T., Zhu, Y., and Masters, P. S. (1995b). Construction of murine coronavirus mutants containing interspecies chimeric nucleocapsid proteins. *J. Virol.* **69:**5475–5484.

Perlman, S. (1998). Pathogenesis of coronavirus-induced infections: Review of pathological and immunological aspects. *Adv. Exp. Med. Biol.* **440:**503–513.

Perlman, S., Ries, D., Bolger, E., Chang, L. J., and Stoltzfus, C. M. (1986). MHV nucleocapsid synthesis in the presence of cycloheximide and accumulation of negative strand MHV RNA. *Virus Res.* **6:**261–272.

Pfleiderer, M., Routledge, E., Herrler, G., and Siddell, S. G. (1991). High level transient expression of the murine coronavirus haemagglutinin-esterase. *J. Gen. Virol.* **72:**1309–1315.

Pfleiderer, M., Routledge, E., and Siddell, S. G. (1990). Functional analysis of the coronavirus MHV-JHM surface glycoproteins in vaccinia virus recombinants. *Adv. Exp. Med. Biol.* **276:**21–31.

Pocock, D. H., and Garwes, D. J. (1977). The polypeptides of haemagglutinating encephalomyelitis virus and isolated subviral particles. *J. Gen. Virol.* **37:**487–499.

Popova, R., and Zhang, X. (2002). The spike but not the hemagglutinin/esterase protein of bovine coronavirus is necessary and sufficient for viral infection. *Virology* **294:**222–236.

Prentice, E., Jerome, W. G., Yoshimori, T., Mizushima, N., and Denison, M. R. (2004). Coronavirus replication complex formation utilizes components of cellular autophagy. *J. Biol. Chem.* **279:**10136–10141.

Raamsman, M. J., Locker, J. K., de Hooge, A., de Vries, A. A., Griffiths, G., Vennema, H., and Rottier, P. J. (2000). Characterization of the coronavirus mouse hepatitis virus strain A59 small membrane protein E. *J. Virol.* **74:**2333–2342.

Regl, G., Kaser, A., Iwersen, M., Schmid, H., Kohla, G., Strobl, B., Vilas, U., Schauer, R., and Vlasak, R. (1999). The hemagglutinin-esterase of mouse hepatitis virus strain S is a sialate-4-*O*-acetylesterase. *J. Virol.* **73:**4721–4727.

Ricard, C. S., Koetzner, C. A., Sturman, L. S., and Masters, P. S. (1995). A conditional-lethal murine coronavirus mutant that fails to incorporate the spike glycoprotein into assembled virions. *Virus Res.* **39:**261–276.

Risco, C., Anton, I. M., Sune, C., Pedregosa, A. M., Martin-Alonso, J. M., Parra, F., Carrascosa, J. L., and Enjuanes, L. (1995). Membrane protein molecules of transmissible gastroenteritis coronavirus also expose the carboxy-terminal region on the external surface of the virion. *J. Virol.* **69:**5269–5277.

Risco, C., Anton, I. M., Enjuanes, L., and Carrascosa, J. L. (1996). The transmissible gastroenteritis coronavirus contains a spherical core shell consisting of M and N proteins. *J. Virol.* **70:**4773–4777.

Risco, C., Muntion, M., Enjuanes, L., and Carrascosa, J. L. (1998). Two types of virus-related particles are found during transmissible gastroenteritis virus morphogenesis. *J. Virol.* **72:**4022–4031.

Robb, J. A., and Bond, C. W. (1979). Pathogenic murine coronaviruses. I. Characterization of biological behavior *in vitro* and virus-specific intracellular RNA of strongly neurotropic JHMV and weakly neurotropic A59V viruses. *Virology* **94:**352–370.

Robbins, S. G., Frana, M. F., McGowan, J. J., Boyle, J. F., and Holmes, K. V. (1986). RNA-binding proteins of coronavirus MHV: Detection of monomeric and multimeric N protein with an RNA overlay-protein blot assay. *Virology* **150:**402–410.

Rossen, J. W., Horzinek, M. C., and Rottier, P. J. (1995). Coronavirus infection of polarized epithelial cells. *Trends Microbiol.* **3:**486–490.

Rottier, P. J. M. (1995). The coronavirus membrane glycoprotein. *In* "The *Coronaviridae*" (S. G. Siddell, ed.), pp. 115–139. Plenum Press, New York.

Rottier, P. J. M., Brandenburg, D., Armstrong, J., van der Zeijst, B., and Warren, G. (1984). Assembly *in vitro* of a spanning membrane protein of the endoplasmic reticulum: The E1 glycoprotein of coronavirus mouse hepatitis virus A59. *Proc. Natl. Acad. Sci. USA* **81:**1421–1425.

Rottier, P. J. M., Horzinek, M. C., and van der Zeijst, B. A. (1981a). Viral protein synthesis in mouse hepatitis virus strain A59-infected cells: Effect of tunicamycin. *J. Virol.* **40:**350–357.

Rottier, P. J. M., Locker, J. K., Horzinek, M. C., and Spaan, W. J. (1990). Expression of MHV-A59 M glycoprotein: Effects of deletions on membrane integration and intracellular transport. *Adv. Exp. Med. Biol.* **276:**127–135.

Rottier, P. J. M., and Rose, J. K. (1987). Coronavirus E1 glycoprotein expressed from cloned cDNA localizes in the Golgi region. *J. Virol.* **61:**2042–2045.

Rottier, P. J. M., Spaan, W. J., Horzinek, M. C., and van der Zeijst, B. A. (1981b). Translation of three mouse hepatitis virus strain A59 subgenomic RNAs in *Xenopus laevis* oocytes. *J. Virol.* **38:**20–26.

Rottier, P. J. M., Welling, G. W., Welling-Wester, S., Niesters, H. G., Lenstra, J. A., and Van der Zeijst, B. A. (1986). Predicted membrane topology of the coronavirus protein E1. *Biochemistry* **25:**1335–1339.

Saeki, K., Ohtsuka, N., and Taguchi, F. (1997). Identification of spike protein residues of murine coronavirus responsible for receptor-binding activity by use of soluble receptor-resistant mutants. *J. Virol.* **71:**9024–9031.

Salanueva, I. J., Carrasco, J. L., and Risco, C. (1999). Structural maturation of the transmissible gastroenteritis coronavirus. *J. Virol.* **73:**7952–7964.

Salzwedel, K., West, J. T., and Hunter, E. (1999). A conserved tryptophan-rich motif in the membrane-proximal region of the human immunodeficiency virus type 1 gp41 ectodomain is important for Env-mediated fusion and virus infectivity. *J. Virol.* **73:**2469–2480.

Sawicki, S. G., and Sawicki, D. L. (1998). A new model for coronavirus transcription. *Adv. Exp. Med. Biol.* **440:**215–219.

Schultze, B., Gross, H. J., Brossmer, R., and Herrler, G. (1991a). The S protein of bovine coronavirus is a hemagglutinin recognizing 9-O-acetylated sialic acid as a receptor determinant. *J. Virol.* **65:**6232–6237.

Schultze, B., and Herrler, G. (1992). Bovine coronavirus uses *N*-acetyl-9-*O*-acetylneuraminic acid as a receptor determinant to initiate the infection of cultured cells. *J. Gen. Virol.* **73:**901–906.

Schultze, B., Wahn, K., Klenk, H. D., and Herrler, G. (1991b). Isolated HE-protein from hemagglutinating encephalomyelitis virus and bovine coronavirus has receptor-destroying and receptor-binding activity. *Virology* **180:**221–228.

Senanayake, S. D., Hofmann, M. A., Maki, J. L., and Brian, D. A. (1992). The nucleocapsid protein gene of bovine coronavirus is bicistronic. *J. Virol.* **66:**5277–5283.

Sethna, P. B., Hofmann, M. A., and Brian, D. A. (1991). Minus-strand copies of replicating coronavirus mRNAs contain antileaders. *J. Virol.* **65:**320–325.

Shen, S., Wen, Z. L., and Liu, D. X. (2003). Emergence of a coronavirus infectious bronchitis virus mutant with a truncated 3b gene: Functional characterization of the 3b protein in pathogenesis and replication. *Virology* **311:**16–27.

Shi, S. T., Huang, P., Li, H. P., and Lai, M. M. (2000). Heterogeneous nuclear ribonucleoprotein A1 regulates RNA synthesis of a cytoplasmic virus. *EMBO J.* **19:**4701–4711.

Siddell, S. G. (ed.) (1995). "The *Coronaviridae*." Plenum Press, New York.

Simmons, G., Reeves, J. D., Rennekamp, A. J., Amberg, S. M., Piefer, A. J., and Bates, P. (2004). Characterization of severe acute respiratory syndrome-associated coronavirus (SARS-CoV) spike glycoprotein-mediated viral entry. *Proc. Natl. Acad. Sci. USA* **101:**4240–4245.

Simon, K., Lingappa, V. R., and Ganem, D. (1988). Secreted hepatitis B surface antigen polypeptides are derived from a transmembrane precursor. *J. Cell Biol.* **107:**2163–2168.

Sims, A. C., Ostermann, J., and Denison, M. R. (2000). Mouse hepatitis virus replicase proteins associate with two distinct populations of intracellular membranes. *J. Virol.* **74:**5647–5654.

Smith, A. R., Boursnell, M. E., Binns, M. M., Brown, T. D., and Inglis, S. C. (1990). Identification of a new membrane-associated polypeptide specified by the coronavirus infectious bronchitis virus. *J. Gen. Virol.* **71:**3–11.

Sola, I., Alonso, S., Sanchez, C., Sanchez-Morgado, J. M., and Enjuanes, L. (2001). Expression of transcriptional units using transmissible gastroenteritis coronavirus derived minigenomes and full-length cDNA clones. *Adv. Exp. Med. Biol.* **494:**447–451.

Spaan, W. J., Rottier, P. J., Horzinek, M. C., and van der Zeijst, B. A. (1981). Isolation and identification of virus-specific mRNAs in cells infected with mouse hepatitis virus (MHV-A59). *Virology* **108:**424–434.

Stern, D. F., and Sefton, B. M. (1982). Coronavirus proteins: Structure and function of the oligosaccharides of the avian infectious bronchitis virus glycoproteins. *J. Virol.* **44:**804–812.

Stohlman, S. A., Baric, R. S., Nelson, G. N., Soe, L. H., Welter, L. M., and Deans, R. J. (1988). Specific interaction between coronavirus leader RNA and nucleocapsid protein. *J. Virol.* **62:**4288–4295.

Stohlman, S. A., Fleming, J. O., Patton, C. D., and Lai, M. M. (1983). Synthesis and subcellular localization of the murine coronavirus nucleocapsid protein. *Virology* **130:**527–532.

Stohlman, S. A., Kyuwa, S., Cohen, M., Bergmann, C., Polo, J. M., Yeh, J., Anthony, R., and Keck, J. G. (1992). Mouse hepatitis virus nucleocapsid protein-specific cytotoxic T lymphocytes are Ld restricted and specific for the carboxy terminus. *Virology* **189:**217–224.

Stohlman, S. A., and Lai, M. M. (1979). Phosphoproteins of murine hepatitis viruses. *J. Virol.* **32:**672–675.

Sturman, L. S., Holmes, K. V., and Behnke, J. (1980). Isolation of coronavirus envelope glycoproteins and interaction with the viral nucleocapsid. *J. Virol.* **33:**449–462.

Sturman, L. S., Ricard, C. S., and Holmes, K. V. (1990). Conformational change of the coronavirus peplomer glycoprotein at pH 8.0 and 37°C correlates with virus aggregation and virus-induced cell fusion. *J. Virol.* **64:**3042–3050.

Sugiyama, K., and Amano, Y. (1981). Morphological and biological properties of a new coronavirus associated with diarrhea in infant mice. *Arch. Virol.* **67:**241–251.

Sui, J., Li, W., Murakami, A., Tamin, A., Matthews, L. J., Wong, S. K., Moore, M. J., Tallarico, A. S., Olurinde, M., Choe, H., Anderson, L. J., Bellini, W. J., Farzan, M., and

Marasco, W. A. (2004). Potent neutralization of severe acute respiratory syndrome (SARS) coronavirus by a human mAb to S1 protein that blocks receptor association. *Proc. Natl. Acad. Sci. USA* **101:**2536–2541.

Surjit, M., Liu, B., Kumar, P., Chow, V. T. K., and Lal, S. K. (2004). The nucleocapsid protein of the SARS coronavirus is capable of self-association through a C-terminal 209 amino acid interaction domain. *Biochem. Biophys. Res. Commun.* **317:**1030–1036.

Suzuki, H., and Taguchi, F. (1996). Analysis of the receptor-binding site of murine coronavirus spike protein. *J. Virol.* **70:**2632–2636.

Swift, A. M., and Machamer, C. E. (1991). A Golgi retention signal in a membrane-spanning domain of coronavirus E1 protein. *J. Cell Biol.* **115:**19–30.

Taguchi, F., and Matsuyama, S. (2002). Soluble receptor potentiates receptor-independent infection by murine coronavirus. *J. Virol.* **76:**950–958.

Tahara, S. M., Dietlin, T. A., Nelson, G. W., Stohlman, S. A., and Manno, D. J. (1998). Mouse hepatitis virus nucleocapsid protein as a translational effector of viral mRNAs. *Adv. Exp. Med. Biol.* **440:**313–318.

Thiel, V., Karl, N., Schelle, B., Disterer, P., Klagge, I., and Siddell, S. G. (2003). Multigene RNA vector based on coronavirus transcription. *J. Virol.* **77:**9790–9798.

Tooze, J., Tooze, S., and Warren, G. (1984). Replication of coronavirus MHV-A59 in sac-cells: Determination of the first site of budding of progeny virions. *Eur. J. Cell Biol.* **33:**281–293.

Tooze, J., Tooze, S. A., and Fuller, S. D. (1987). Sorting of progeny coronavirus from condensed secretory proteins at the exit from the *trans*-Golgi network of AtT20 cells. *J. Cell Biol.* **105:**1215–1226.

Tresnan, D. B., Levis, R., and Holmes, K. V. (1996). Feline aminopeptidase N serves as a receptor for feline, canine, porcine, and human coronaviruses in serogroup I. *J. Virol.* **70:**8669–8674.

Tripet, B., Howard, M. W., Jobling, M., Holmes, R. K., Holmes, K. V., and Hodges, R. S. (2004). Structural characterization of the SARS-coronavirus spike S fusion protein core. *J. Biol. Chem.* **279:**20836–20849.

Tsai, J. C., Zelus, B. D., Holmes, K. V., and Weiss, S. R. (2003). The N-terminal domain of the murine coronavirus spike glycoprotein determines the CEACAM1 receptor specificity of the virus strain. *J. Virol.* **77:**841–850.

Tung, F. Y., Abraham, S., Sethna, M., Hung, S. L., Sethna, P., Hogue, B. G., and Brian, D. A. (1992). The 9-kDa hydrophobic protein encoded at the 3′ end of the porcine transmissible gastroenteritis coronavirus genome is membrane-associated. *Virology* **186:**676–683.

van Berlo, M. F., van den Brink, W. J., Horzinek, M. C., and van der Zeijst, B. A. (1987). Fatty acid acylation of viral proteins in murine hepatitis virus-infected cells: Brief report. *Arch. Virol.* **95:**123–128.

van der Meer, Y., Snijder, E. J., Dobbe, J. C., Schleich, S., Denison, M. R., Spaan, W. J., and Locker, J. K. (1999). Localization of mouse hepatitis virus nonstructural proteins and RNA synthesis indicates a role for late endosomes in viral replication. *J. Virol.* **73:**7641–7657.

van der Most, R. G., Bredenbeek, P. J., and Spaan, W. J. (1991). A domain at the 3′ end of the polymerase gene is essential for encapsidation of coronavirus defective interfering RNAs. *J. Virol.* **65:**3219–3226.

van Genderen, I. L., Godeke, G. J., Rottier, P. J., and van Meer, G. (1995). The phospholipid composition of enveloped viruses depends on the intracellular membrane through which they bud. *Biochem. Soc. Trans.* **23:**523–526.

Vennema, H. (1999). Genetic drift and genetic shift during feline coronavirus evolution. *Vet. Microbiol.* **69:**139–141.

Vennema, H., Godeke, G. J., Rossen, J. W., Voorhout, W. F., Horzinek, M. C., Opstelten, D. J., and Rottier, P. J. (1996). Nucleocapsid-independent assembly of coronavirus-like particles by co-expression of viral envelope protein genes. *EMBO J.* **15:**2020–2028.

Vennema, H., Heijnen, L., Zijderveld, A., Horzinek, M. C., and Spaan, W. J. (1990a). Intracellular transport of recombinant coronavirus spike proteins: Implications for virus assembly. *J. Virol.* **64:**339–346.

Vennema, H., Poland, A., Foley, J., and Pedersen, N. C. (1998). Feline infectious peritonitis viruses arise by mutation from endemic feline enteric coronaviruses. *Virology* **243:**150–157.

Vennema, H., Rottier, P. J., Heijnen, L., Godeke, G. J., Horzinek, M. C., and Spaan, W. J. (1990b). Biosynthesis and function of the coronavirus spike protein. *Adv. Exp. Med. Biol.* **276:**9–19.

Vlasak, R., Luytjes, W., Leider, J., Spaan, W., and Palese, P. (1988a). The E3 protein of bovine coronavirus is a receptor-destroying enzyme with acetylesterase activity. *J. Virol.* **62:**4686–4690.

Vlasak, R., Luytjes, W., Spaan, W., and Palese, P. (1988b). Human and bovine coronaviruses recognize sialic acid-containing receptors similar to those of influenza C viruses. *Proc. Natl. Acad. Sci. USA* **85:**4526–4529.

Wang, Y., and Zhang, X. (1999). The nucleocapsid protein of coronavirus mouse hepatitis virus interacts with the cellular heterogeneous nuclear ribonucleoprotein A1 *in vitro* and *in vivo*. *Virology* **265:**96–109.

Wege, H., Nagashima, K., and ter Meulen, V. (1979). Structural polypeptides of the murine coronavirus JHM. *J. Gen. Virol.* **42:**37–47.

Weisz, O. A., Swift, A. M., and Machamer, C. E. (1993). Oligomerization of a membrane protein correlates with its retention in the Golgi complex. *J. Cell Biol.* **122:**1185–1196.

Wilbur, S. M., Nelson, G. W., Lai, M. M., McMillan, M., and Stohlman, S. A. (1986). Phosphorylation of the mouse hepatitis virus nucleocapsid protein. *Biochem. Biophys. Res. Commun.* **141:**7–12.

Wilhelmsen, K. C., Leibowitz, J. L., Bond, C. W., and Robb, J. A. (1981). The replication of murine coronaviruses in enucleated cells. *Virology* **110:**225–230.

Williams, R. K., Jiang, G. S., and Holmes, K. V. (1991). Receptor for mouse hepatitis virus is a member of the carcinoembryonic antigen family of glycoproteins. *Proc. Natl. Acad. Sci. USA* **88:**5533–5536.

Wong, S. K., Li, W., Moore, M. J., Choe, H., and Farzan, M. (2004). A 193-amino acid fragment of the SARS coronavirus S protein efficiently binds angiotensin-converting enzyme 2. *J. Biol. Chem.* **279:**3197–3201.

Woo, K., Joo, M., Narayanan, K., Kim, K. H., and Makino, S. (1997). Murine coronavirus packaging signal confers packaging to nonviral RNA. *J. Virol.* **71:**824–827.

Woods, R. D. (2001). Efficacy of a transmissible gastroenteritis coronavirus with an altered ORF-3 gene. *Can. J. Vet. Res.* **65:**28–32.

Wurm, T., Chen, H., Hodgson, T., Britton, P., Brooks, G., and Hiscox, J. A. (2001). Localization to the nucleolus is a common feature of coronavirus nucleoproteins, and the protein may disrupt host cell division. *J. Virol.* **75:**9345–9356.

Wurzer, W. J., Obojes, K., and Vlasak, R. (2002). The sialate-4-*O*-acetylesterases of coronaviruses related to mouse hepatitis virus: A proposal to reorganize group 2 *Coronaviridae*. *J. Gen. Virol.* **83:**395–402.

Xu, Y., Liu, Y., Lou, Z., Qin, L., Li, X., Bai, Z., Pang, H., Tien, P., Gao, G. F., and Rao, Z. (2004). Structural basis for coronavirus-mediated membrane fusion: Crystal structure of MHV spike protein fusion core. *J. Biol. Chem.* **279:**30514–30522.

Yamada, Y. K., Yabe, M., Ohtsuki, T., and Taguchi, F. (2000). Unique N-linked glycosylation of murine coronavirus MHV-2 membrane protein at the conserved O-linked glycosylation site. *Virus Res.* **66:**149–154.

Yeager, C. L., Ashmun, R. A., Williams, R. K., Cardellichio, C. B., Shapiro, L. H., Look, A. T., and Holmes, K. V. (1992). Human aminopeptidase N is a receptor for human coronavirus 229E. *Nature* **357:**420–422.

Ying, W., Hao, Y., Zhang, Y., Peng, W., Qin, E., Cai, Y., Wei, K., Wang, J., Chang, G., Sun, W., Dai, S., Li, X., Zhu, Y., Li, J., Wu, S., Guo, L., Dai, J., Wan, P., Chen, T., Du, C., Li, D., Wan, J., Kuai, X., Li, W., Shi, R., Wei, H., Cao, C., Yu, M., Liu, H., Dong, F., Wang, D., Zhang, X., Qian, X., Zhu, Q., and He, F. (2004). Proteomic analysis on structural proteins of severe acute respiratory syndrome coronavirus. *Proteomics* **4:**492–504.

Yokomori, K., Asanaka, M., Stohlman, S. A., Makino, S., Shubin, R. A., Gilmore, W., Weiner, L. P., Wang, F. I., and Lai, M. M. (1995). Neuropathogenicity of mouse hepatitis virus JHM isolates differing in hemagglutinin-esterase protein expression. *J Neurovirol.* **1:**330–339.

Yokomori, K., Baker, S. C., Stohlman, S. A., and Lai, M. M. C. (1992). Hemagglutinin-esterase specific monoclonalantibodies alter the neuropathogenicity of mouse hepatitis virus. *J. Virol.* **66:**2865–2874.

Yokomori, K., Banner, L. R., and Lai, M. M. (1991). Heterogeneity of gene expression of the hemagglutinin-esterase (HE) protein of murine coronaviruses. *Virology* **183:**647–657.

Yokomori, K., La Monica, N., Makino, S., Shieh, C. K., and Lai, M. M. (1989). Biosynthesis, structure, and biological activities of envelope protein gp65 of murine coronavirus. *Virology* **173:**683–691.

Yokomori, K., Stohlman, S. A., and Lai, M. M. (1993). The detection and characterization of multiple hemagglutinin-esterase (HE)-defective viruses in the mouse brain during subacute demyelination induced by mouse hepatitis virus. *Virology* **192:**170–178.

Yoo, D., Graham, F. L., Prevec, L., Parker, M. D., Benko, M., Zamb, T., and Babiuk, L. A. (1992). Synthesis and processing of the haemagglutinin-esterase glycoprotein of bovine coronavirus encoded in the E3 region of adenovirus. *J. Gen. Virol.* **73:**2591–2600.

Yoshikura, H., and Taguchi, F. (1978). Mouse hepatitis virus strain MHV-S: Formation of pseudotypes with a murine leukemia virus envelope. *InterVirology* **10:**132–136.

Yu, X., Bi, W., Weiss, S. R., and Leibowitz, J. L. (1994). Mouse hepatitis virus gene 5b protein is a new virion envelope protein. *Virology* **202:**1018–1023.

Yuan, K., Yi, L., Chen, J., Qu, X., Qing, T., Rao, X., Jiang, P., Hu, J., Xiong, Z., Nie, Y., Shi, X., Wang, W., Ling, C., Yin, X., Fan, K., Lai, L., Ding, M., and Deng, H. (2004). Suppression of SARS-CoV entry by peptides corresponding to heptad regions on spike glycoprotein. *Biochem. Biophys. Res. Commun.* **319:**746–752.

Zelus, B. D., Schickli, J. H., Blau, D. M., Weiss, S. R., and Holmes, K. V. (2003). Conformational changes in the spike glycoprotein of murine coronavirus are induced at 37 °C either by soluble murine CEACAM1 receptors or by pH 8. *J. Virol.* **77:**830–840.

Zhang, X., Hinton, D. R., Park, S., Parra, B., Liao, C. L., Lai, M. M., and Stohlman, S. A. (1998). Expression of hemagglutinin/esterase by a mouse hepatitis virus coronavirus defective-interfering RNA alters viral pathogenesis. *Virology* **242:**170–183.

Zhao, X., Shaw, K., and Cavanagh, D. (1993). Presence of subgenomic mRNAs in virions of coronavirus IBV. *Virology* **196:**172–178.

Zhou, M., and Collisson, E. W. (2000). The amino and carboxyl domains of the infectious bronchitis virus nucleocapsid protein interact with 3′ genomic RNA. *Virus Res.* **67:**31–39.

Zhou, M., Williams, A. K., Chung, S. I., Wang, L., and Collisson, E. W. (1996). The infectious bronchitis virus nucleocapsid protein binds RNA sequences in the 3′ terminus of the genome. *Virology* **217:**191–199.

Zhu, J., Xiao, G., Xu, Y., Yuan, F., Zheng, C., Liu, Y., Yan, H., Cole, D. K., Bell, J. I., Rao, Z., Tien, P., and Gao, G. F. (2004). Following the rule: Formation of the 6-helix bundle of the fusion core from severe acute respiratory syndrome coronavirus spike protein and identification of potent peptide inhibitors. *Biochem. Biophys. Res. Commun.* **319:**283–288.

Ziebuhr, J., Snijder, E. J., and Gorbalenya, A. E. (2000). Virus-encoded proteinases and proteolytic processing in the Nidovirales. *J. Gen. Virol.* **81:**853–879.